UNIVERSIDADE DA BEIRA INTERIOR
Ciências

Biosynthesis scale-up of human soluble catechol-*O*-methyltransferase

Guilherme Manuel Palha Ruivo do Espírito Santo

Dissertação para obtenção do Grau de Mestre em
Biotecnologia
(2º ciclo de estudos)

Orientador: Prof. Doutor Luís Passarinha
Co-Orientadora: Profª. Doutora Filomena Silva

Covilhã, outubro de 2013

Acknowledgments

First of all, I would like to express my sincere gratitude to Professor Doctor Luís Passarinha and Professor Doctor Filomena Silva for all their guidance, expertise, and trust. I really appreciate their help, which was crucial for the development of this work, and their vast knowledge, criticism and suggestions.

I would also like to express my gratitude to Augusto, whose expertise, companionship, advice and encouragement made my work much more pleasant and easy.

Furthermore, I would like to thank to all people involved in the Health Sciences Research Centre of the University of Beira Interior, particularly to the Biotechnology and Biomolecular Sciences group.

Finally, I am extremely thankful to all my friends and family for their unconditional support and encouragement through all this time.

Resumo

A proteína catecol-*O*-metiltransferase (COMT, CE 2.1.1.6) foi descrita pela primeira vez em 1958. É uma enzima metiltransferase dependente da S-adenosil-L-metionina (SAM) que catalisa a metilação de substratos catecólicos (catecolaminas, catecolestrogénios). Esta enzima desempenha várias funções importantes no organismo, funcionando como uma barreira entre o sangue e diversos orgãos, através da eliminação de catecóis biológicamente activos ou tóxicos. A enzima COMT desempenha ainda uma função particularmente importante no cérebro, onde participa no metabolismo do neurotransmissor dopamina, pelo que o seu papel nas doenças neurodegenerativas é extremamente relevante, nomeadamente na doença de Parkinson. Esta deonça é caracterizada pela perda progressive de neurónios libertadores de dopamina, levando a uma diminuição acentuada dos níveis deste neurotransmissor no cérebro. Nesta patologia, um dos principais alvos terapêuticos é a enzima COMT, já que a sua ação é indesejável nos pacientes portadores desta doença. Nos últimos anos têm vindo a ser desenvolvidos vários inibidores desta enzima para o tratamento da doença de Parkinson, e há um grande interesse em desenvolver novos inibidores mais eficazes. Para tal, são necessárias grandes quantidades de COMT numa forma activa, e a melhor maneira de o conseguir é a sua produção em larga escala através de processos biotecnológicos. Neste trabalho é proposto um processo de produção em larga escala da isoforma solúvel da COMT, utilizando o sistema de expressão *Escherichia coli* para a biosíntese da isoforma solúvel desta proteína e testando várias condições de fermentação, com o objectivo de estabelecer um processo de fermentação descontínuo com posterior fornecimento de substrato, controlando vários parâmetros durante esta fase. As condições de fermentação escolhidas, após terem sido testadas em processos de fermentação contínuos, foram uma percentagem de oxigénio dissolvido de 20%, uma concentração de 20 g/L das fontes de carbono e azoto (glicerol e triptona, respectivamente), e por fim, um perfil de adição de substrato no processo de alimentação de 1 g glicerol/L/h. Os resultados finais foram uma densidade óptica máxima de aproximadamente 50 e uma actividade enzimática especifica de 442.34 nmol/h/mg.

Palavras-chave

COMT solúvel humana, Doença de Parkinson, produção em larga escala.

Resumo alargado

A catecol-*O*-metiltransferase (COMT, CE 2.1.1.6) foi descrita e purificada pela primeira vez em 1958. É uma enzima metiltransferase que cataliza a transferência do grupo metil da S-adenosyl-L-metionina (SAM) para um dos grupos hidroxilo do substrato catecólico (incluindo catecolaminas e catecolestrogéneos) na presença do ião Mg^{2+}.

Esta enzima existe sob a forma de duas isoformas, uma solúvel (SCOMT) localizada no citosol e outra associada a membranas plasmáticas (MBCOMT), ambas codificadas pelo mesmo gene (localizado no cromossoma 22) a partir de dois promotores. Ambas são expressas na maioria dos tecidos humanos, excepto no cérebro, onde a MBCOMT é a isoforma dominate.

A função geral da COMT é a eliminação de catecóis biologicamente activos ou tóxicos, funcionando como uma barreira desintoxicante entre o sangue e vários tecidos. Além disso, esta enzima desempenha um papel fundamental no metabolismo do neurotransmissor dopamina, associado a várias doenças neurodegenerativas.

Uma destas doenças é a doença de Parkinson, uma das doenças neurodegenerativas mais comuns, afectando cerca de 6 milhões de pessoas a nível mundial, e dados apontam para que esse número duplique nos próximos 20 anos. Esta doença foi descrita pela primeira vez em 1817 por James Parkinson, e caracteriza-se pela perda progressiva e profunda de neurónios libertadores de dopamina, levando a uma diminuição dos níveis deste transmissor no cérebro.

Devido a esta diminuição nos níveis de dopamina, as estratégias farmacológicas mais comuns para esta patologia têm como objectivo repor esses níveis, pela administração de levodopa, uma molécula que depois de metabolizada no cérebro dá origem à dopamina, ou de moléculas agonistas da dopamina.

Estes tratamentos, no entanto, são muito limitados, e posteriormente surgiram novas terapias que os complementam, como por exemplo a administração de inibidores da COMT. Tendo em conta a ligação entre a COMT e o metabolismo da dopamina, os inibidores da COMT assumem extrema importância para atenuar os efeitos indesejáveis desta proteína na patologia.

Os primeiros inibidores desenvolvidos, são tóxicos, pouco efectivos *in vivo* e/ou pouco selectivos. Há portanto um grande interesse científico no desenvolvimento de novos e melhorados inibidores, e para tal são necessárias elevadas quantidades de COMT na sua forma activa.

Assim sendo, o principal objectivo deste trabalho é a produção a larga escala da isoforma solúvel desta enzima, usando a estirpe *E. coli* BL21 (DE3) como sistema de expressão para a

biossíntese da COMT. Foi portanto desenvolvido um processo de fermentação descontínuo com fornecimento de substrato ("Fed-batch") em bioreactores de bancada.

Partindo de duas condições de fermentação anteriormente optimizadas pelo nosso grupo de investigação (Temperatura, 40°C e ph 6.5), várias outras condições foram testadas, nomeadamente a percentagem de oxigénio dissolvido, a concentração das fontes de carbono e azoto e os perfis de adição de substrato; e três parâmetros da cultura celular foram analisados durante o processo: concentração de fonte de carbono, viabilidade celular e actividade enzimática.

As condições de fermentação escolhidas, após terem sido testadas em processos de fermentação contínuos, foram uma percentagem de oxigénio dissolvido de 20%, uma concentração de 20 g/L das fontes de carbono e azoto (glicerol e triptona, respectivamente), e por fim, um perfil de adição de substrato no processo de alimentação de 1 g glicerol/L/h.

Os resultados finais foram uma densidade óptica máxima de aproximadamente 50 e uma actividade enzimática especifica de 442.34 nmol/h/mg.

Abstract

Catechol-*O*-methyltransferase (COMT, EC 2.1.1.6) was first described in 1958. It is a S-adenosyl-L-methionine (SAM) dependent methyltransferase which catalyses the methylation of catechol substrates (catecholamines, catecholestrogens). This enzyme has several important functions in the body, acting as a barrier between the blood and various organs, through the elimination of toxic or biologically active catechols. COMT plays a particularly important role in the brain, where it participates in the metabolism of the neurotransmitter dopamine, and so its role in neurodegenerative diseases is extremely relevant, especially in Parkinson's disease. In recent years, several COMT inhibitors have been developed for Parkinson's disease treatment, and there is considerable interest in developing new and more effective inhibitors. To do so, large amounts of COMT in an active form are necessary, and the best way to achieve this is by up-scaling its production through biotechnological processes. In this work, we propose a fed-batch process for biosynthesis scale-up of the soluble isoform of COMT, using an *Escherichia coli* expression system for the production of the soluble isoform of this protein, testing various fermentation conditions and controlling various parameters during the process. After several different batch and fed-batch experiments, the selected fermentation conditions were 20% dissolved oxygen, an initial batch concentration of 20 g/L of glycerol and tryptone, and a constant feed of 1 g glycerol/L/h, achieving a final specific COMT activity of 442.34 nmol/h/mg. Cell viability was monitored by flow cytometry and glycerol concentration by an HPLC system.

Keywords

Human SCOMT, Parkinson’s disease, fed-batch, biosynthesis scale-up.

Table of Contents

List of Figures

List of Tables

List of Acronyms

3-MT	3-methoxytyramine
AADC	aromatic amino acid decarboxylase
AD	Alzheimer's disease
BOX	Bis-(1,3-dibutylbarbituric acid)trimethine oxonol
BSA	Bovine serum albumin
COMT	Catechol-*O*-methyltransferase
DAT	dopamine transporter
DCW	Dry cell weight
DNC	3,5-dinitrocatechol
DTT	Dithiotreitol
EDTA	ethylenediamine tetraacetic acid
EGTA	ethylene glicol tetraacetic acid
HPLC	High performance liquid chromatography
hSCOMT	human SCOMT
HVA	homovanillic acid
IPTG	Isopropyl-b-D-thiogalactopyranoside
MAO-B	Monoamine oxidase B
MBCOMT	Membrane-bound COMT
OD	Optical density
OSA	Sodium octyl sulphate
PD	Parkinson's disease
PFC	Prefrontal cortex
PI	Propidium iodide
PVA	Potato virus A
SAM	S-adenosyl-L-methionine
SCOMT	Soluble COMT

Justification and Objectives

Cathecol-*O*-methyltransferase (COMT) is a methyltrasnferase enzyme that catalyzes the transfer of the methyl group from S-adenosyl-L-methionine (SAM) to one of the methyl groups of a catechol substrate. One of these substrates is the neurotransmitter dopamine, which is associated to several neurodegenerative diseases, such as Parkinson's disease.

Given the important role played by COMT in the metabolism of dopamine, this enzyme is directly related with Parkinson's disease, being one of the therapeutical targets for the treatment of this disease.

For this reason, there is a great interest in the development of COMT inhibitors for administration in patients with Parkinson's disease, and for that, high quantities of the active form of COMT are necessary.

Therefore, the goal of this work was the optimization of soluble COMT biosynthesis, via a fed-batch process applied to bench-top bioreactors, optimizing several culture conditions while monitoring substrate concentration, cell viability and enzymatic activity.

Chapter 1 - Introduction

1.1 – General overlook of catechol-O-methyltransferase

Catechol-*O*-methyltransferase (COMT, EC 2.1.1.6) was first described and partly purified in 1958 by Axelrod and coworkers [1, 2]. COMT is a methyltransferase enzyme that catalyzes the transfer of the methyl group from S-adenosyl-L-methionine (SAM) to one of the hydroxyl groups of the catechol substrate (including catecholamine neurotransmitters and catechol estrogens) in the presence of Mg^{2+} [3]. This methylation reaction is a sequentially ordered mechanism, with SAM being the first to bind to the enzyme, followed by the Mg^{2+} ion and finally the substrate [3].

The enzyme exists as two isoforms: a soluble, cytosolic protein (SCOMT) and a membrane-bound protein (MBCOMT) [4], both coded by the same gene (located in chromosome 22), from two promoters. Most of the human tissues express both transcripts, except for the brain, where MBCOMT is the dominant allozyme, while SCOMT is only present in small amounts [5]. In fact, western blot analysis showed that in human brain 70% of the COMT polypeptides were MBCOMT, and only 30% were SCOMT [3].

SCOMT contains 221 amino acids, and has a molecular mass of 24.4 kDa [3]. The membrane-bound isoform has an additional 50 hydrophobic residues at the N-terminus, 20 of them acting as the membrane-spanning region, and a molecular mass of 30 kDa [3, 4, 5].

The general function of COMT is the elimination of biologically active or toxic catechols and other metabolites, acting as a detoxifying barrier between the blood and other tissues, and it is particularly active in the liver, kidneys and gastrointestinal tract. It is also present in the placenta during the first trimester of pregnancy for embryo protection [3].

This enzyme plays a particularly important role in the metabolism of catecholamines, especially in the breakdown of the neurotransmitter dopamine [5], thus being extremely important in the prefrontal cortex (PFC) because of the relative lack of dopamine transporters in this region [6], as later explained.

1.1.1 – The V108M polymorphism

Human COMT contains a common polymorphism at residue 108, which can be either a valine (V) or a methionine (M), the second having decreased protein levels and lower structural stability, and being more susceptible to oxidation and unfolding [3, 4, 6, 7, 8]. Since the alleles are codominant, there is a trimodal distribution of COMT activity in human populations: 108V homozygotes (higher COMT activity), 108M homozygotes (lower COMT activity) and heterozygotes (intermediate activity) [3, 5]. Approximately 25% of United States and Northern European Caucasians are homozygous for the 108M allele, and it is much less common in African and Asian populations. It has been linked to increased risk for breast cancer [9], obsessive-compulsive disorder [10], schizophrenia [11, 12] and increased sensitivity to pain [13], but also with improved prefrontal cognitive function [14].

This polymorphism hasn't been found in any other species, therefore the 108M variant may be specific to humans. It appears that COMT activity has decreased during evolution, which may reflect the beneficial effect of lowered COMT activity on prefrontal function. All this complex associations and the referred problems associated with this variant possibly underlie the persistence of both alleles in human race [5]. Because there is only one COMT gene without any known tissue-specific variants, it is likely that the V108M polymorphism leads to functional alterations of COMT in all tissues [3], hence its importance when studying this enzyme.

1.1.2 – Crystal structure of human SCOMT

The structure of human SCOMT (hSCOMT) has been determined with the enzyme complexed with Mg^{2+}, SAM and the inhibitor 3,5-dinitrocatechol (DNC) [4]. The 108V SCOMT structure was obtained via X-Ray diffraction data (based on rat COMT structure [15]) to a 1.98 Å resolution, and this structure was then used as the initial phasing model for the isomorphous 108M SCOMT crystal, set to a 1.30 Å resolution [4].

hSCOMT is composed of a seven-stranded β-sheet core sandwiched between two sets of α-helices (Fig. 1). This structure is characteristic of the SAM-dependent methyltransferase fold family [16], differing only in the presence of an extended loop between β-strands 6 and 7 which forms part of the catechol-binding site [4]. The cofactor SAM, Mg^{2+} and DNC all bind in shallow clefts on the protein surface (Fig. 1). The molecule SAM interacts with conserved motifs along the first half of the core β-sheet (Fig. 1) [4].

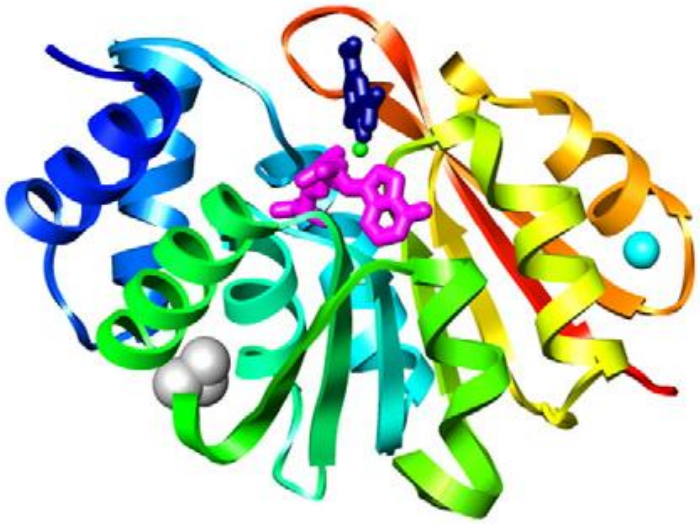

Figure 1 - Crystal structure of human 108V SCOMT (adapted from [4]). Ribbon diagrams colored from blue (N-terminus) to red (C-terminus). SAM (magenta), DNC (dark blue) are shown in stick representation. K^+ (cyan), Mg^{2+} (green) and the side chain of residue V108 (gray) are shown in space-filling representation.

The catechol-binding site is a shallow pocket defined by five residues, including "gatekeeper" residues W38 and P174, which hold the substrate in the correct orientation for methylation. Mg^{2+} is coordinated in the active site by the side chains of three residues, the two hydroxyl groups of the catechol substrate, and a water molecule [4].

Human SCOMT contains seven cysteine residues, three of which (C95, C173, C188) are not conserved in the rat enzyme. C95 is located in the catechol binding site, and C173 is located next to the P174 "gatekeeper" residue. The crystal structure reveals that four of the seven residues are located in surface loops with their sulfur atoms exposed to solvent, making them potential sites for intermolecular disulfide bond formation [4].

There are very few structural differences between the two human holoproteins, and the orientations of SAM, Mg^{2+} and DNC, as well as their interaction with residues within the SAM and catechol binding sites are virtually identical. However, intramolecular packing deviations are present in the vicinity of the polymorphic residue, due to its location in a surface loop between helix α5 and strand ß3, both of which have SAM binding residues at their distal ends. These conformational changes may be restricted by SAM's ability to stabilize both secondary and tertiary structures of 108M COMT [4].

1.2 –COMT in catecholamine metabolism

As mentioned above, COMT plays a particularly important role in the breakdown of catecholamines, despite historically being considered of minor importance compared with that of monoamine oxidase [5]. In fact, mounting evidence suggests that COMT is extremely important for the breakdown of dopamine, particularly in the PFC (Fig. 2) [5]

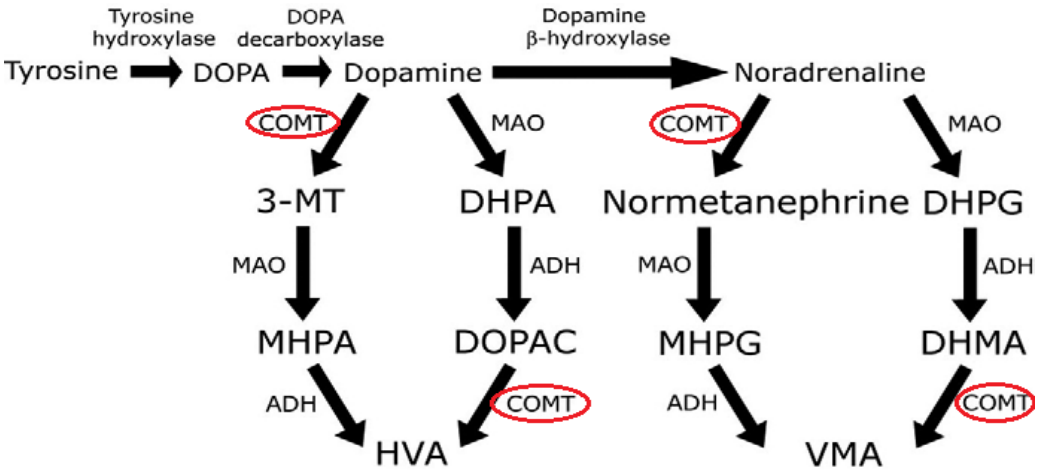

Figure 2- Synthesis and metabolism of dopamine into homovanilic acid (HVA) and noradrenaline into vanillylmandelic acid (VMA) (adapted from [5]).

As seen in Fig. 2, COMT takes part in several steps of this process. First, the *O*-methylation of dopamine by COMT forms 3-methoxytyramine (3-MT), which is the major metabolite of released dopamine in rat PFC, suggesting that this reaction is a prominent pathway in this region [5]. Also, studies using COMT knockout mice revealed an almost 3-fold increase of dopamine levels in the frontal cortex of males, with no changes in other brain regions or in noradrenaline levels [3, 5, 17]. In support of these findings, Tunbridge and coworkers showed that the administration of the specific and brain-penetrant COMT inhibitor tolcapone greatly increases extracellular dopamine, but not noradrenaline, in rat PFC [18].

Thus, it seems that COMT is important for regulating dopamine but not noradrenaline levels in the PFC, although the underlying mechanism remains unclear. Also, despite the complete lack of COMT gene and protein, residual homovanillic acid (HVA) levels were detectable in several brain areas, pointing to the possibility that there is still an unidentified methylation pathway in the brain [5, 18].

Besides PFC, the only other brain region in which the importance of COMT for modulating catecholamine function has been extensively studied is the striatum, where this enzyme plays a minor role in the removal of dopamine (Fig. 2).

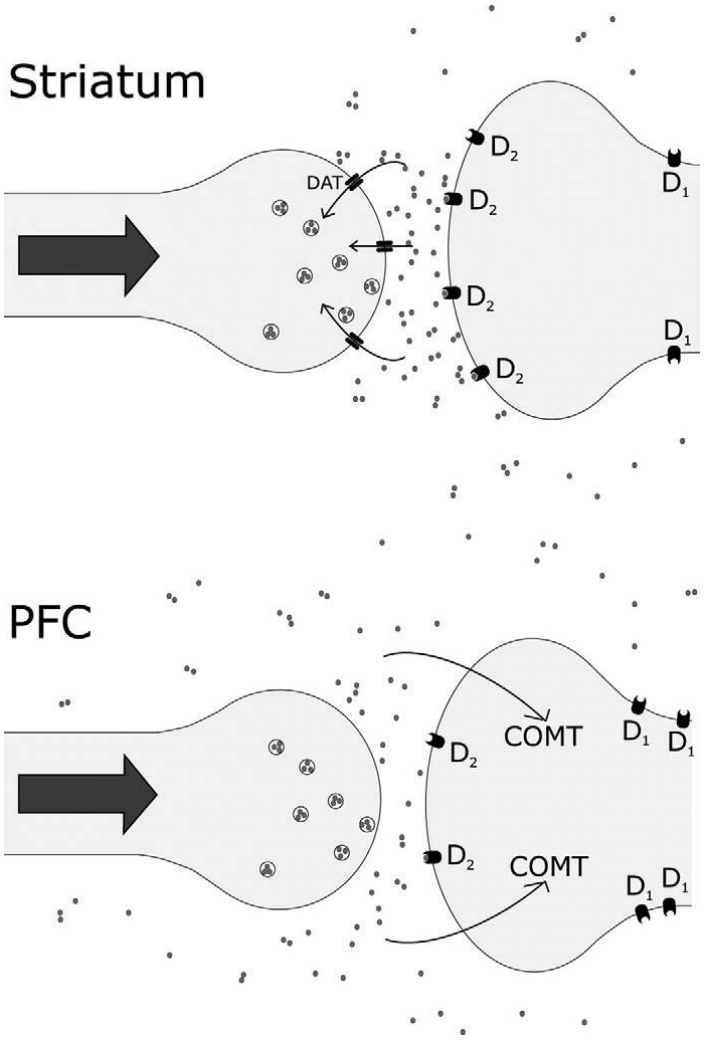

Figure 3- Dopaminergic transmission in PFC and striatum (adapted from [5]).

The critical relevance of COMT in the PFC is due to the relative lack of dopamine transporter (DAT) in this region, compared to the striatum. Since this transporter is responsible for removing dopamine from the synaptic cleft, it is likely that PFC dopamine is able to diffuse to extra synaptic sites, increasing the likelihood to be degraded by COMT during this process [5]. Since the DAT in the striatum is more abundant than in PFC, dopamine is more effectively removed from the synaptic cleft, with COMT playing at most a minor role (Fig. 2).

As mentioned above, the polymorphism in residue 108 leads to two different results: when this residue is a valine, an increase in COMT activity is observed, which results in reduced prefrontal dopamine levels, subsequently leading to an increased regulation of striatal dopamine activity; however, when the residue is a methionine, a significant reduction in COMT's enzymatic activity is observed [3, 5, 6, 19]. Therefore, the valine/methionine polymorphism has been reported as a risk factor for several psychiatric disorders.

1.3 –COMT and neurodegenerative diseases

Neurodegenerative diseases result from the gradual and progressive loss of neural cells, leading to nervous system dysfunction [20]. Known risk factors for neurodegenerative diseases include certain genetic polymorphysms [19, 21, 22], increasing age [20], among others. These are incurable and debilitating diseases that cause problems with movement (ataxias) or mental functioning (dementias), with dementias being responsible for the greatest burden of disease [8, 20, 23].

1.3.1 – COMT and Alzheimer's disease

Alzheimer's disease (AD) is the most common type of dementia, and is ultimately fatal. It was first identified more than 100 years ago, and although research has revealed a great deal of information about AD, the precise brain changes that trigger the development of the disease, and the order in which they occur, remain largely unknown.

AD is characterized by a variety of behavioral and psychological symptoms, which are the most distressing manifestations of dementia and result in considerable social and economic costs [8]. These psychotic symptoms denote a severe phenotype, characterized by rapid cognitive decline, hostility and aggressive behavior [6].

In recent years, it has been suggested that an underlying genetically distinct condition is present in AD's psychotic symptoms, with the genes involved in dopamine metabolism being considered as potential candidates [19] for this genetic condition, which could imply the involvement of COMT, as this enzyme plays a crucial role in this process. Thus, the presence of valine (H allele = high activity) in the coding sequence of this protein corresponds, in a dose dependent manner, to reduced prefrontal dopamine levels [6], and, therefore, the COMT gene could be a susceptibility gene for AD related psychosis, with the valine/methionine genetic polymorphism being reported as a risk factor psychosis susceptibility in AD [19, 24].

1.3.2 – COMT and Parkinson's disease

Another neurodegenerative disease that has been linked to COMT is Parkinson's disease (PD). PD is the most common neurodegenerative movement disorder, affecting 1-2% of the

population over 60 years old (about 6 million people worldwide) and data indicate that this number is expected to double within the next two decades [23]. This disease was first described by James Parkinson in 1817, and it is characterized by progressive and profound loss of dopaminergic neurons, with the presence of Lewy bodies (protein aggregates) in surviving neurons [25]. Symptoms of PD include motor impairment (resting tremor, rigidity) and non-motoric symptoms (cognitive and psychiatric problems), and, despite extensive in the field, neither the cause nor the mechanisms underlying the condition have been firmly established [23, 25].

Despite the above mentioned lack of certainties regarding the causes of PD, it is known that the lack of dopamine may lead to PD (due to a loss of dopamine-producing neurons) [25, 26], and so, levodopa (a dopamine precursor, its administration leads to an increment in dopamine levels) and dopamine agonists (chemicals that mimic dopamine action) are currently the drugs of choice for PD when a significant symptomatic effect needs to be achieved [27].

Unlike dopamine, levodopa crosses the blood-brain barrier and is then decarboxylated to dopamine by aromatic amino acid decarboxylase (AADC) and released by presynaptic terminals in the stratium, replenishing the dopaminergic deficiency [28].

The administration of levodopa is the most common dopaminergic therapy used [27], but about 40% of patients subjected to this treatment may suffer from a “wearing-off” effect, when previously controlled symptoms re-emerge towards the end of the dosing interval, or “on-off” effects, characterized by unpredictable, abrupt fluctuations in the motor system from controlled to uncontrolled states [29, 30]. It was thought that if levodopa was used for a long time, dopamine metabolism produced reactive oxygen species and toxic quinine species [31], but this toxicity concerns have now been mostly discarded [27]. However, the bioavailability of this drug is low, since, when taken orally, levodopa is quickly decarboxylated before reaching the brain, meaning that only a small proportion (about 1% of the administrated dose [28]) of this drug is able to reach the central nervous system [27].

The combination of levodopa with a peripheral AADC inhibitor (unable to enter the central nervous system) remains the most effective treatment for PD, however, even with this combination, only 5 to 10% of administrated levodopa reaches the brain [28]

In order to overcome these limitations, levodopa should be administrated as a formulation that effectively increases its bioavailability [27], and an adjuvant therapy, such as dopamine agonists, is often initiated [29].

Dopamine agonists have also been widely used as an initial therapy for PD because of their effectiveness and their increased capacity to reduce the risk of motor complications when compared with levodopa. However, 50% of the patients initiated on this treatment required

the administration of levodopa to maintain symptom control, and dopamine agonists can also cause behavioral side effects [27].

The use of COMT or monoamine oxidase B (MAO-B, another enzyme involved in the degradation of dopamine and noradrenaline) inhibitors plus levodopa is superior at reducing PD symptoms, compared to using levodopa alone, in patients with advanced PD. They are especially useful amongst patients experiencing fluctuations from levodopa therapy that may already be on dopamine agonists [29].

Another option for complementary levodopa therapy is the administration of MAO-B or COMT inhibitors [27, 29, 31]. Patients receiving these treatments exhibit significant improvement in their PD symptoms, decreasing the necessary levodopa dose [29]. However, studies evaluating MAO-B inhibitors are still scarce, and these molecules carry the risk of many different interactions compared to COMT inhibitors [29].

1.3.2.1 – COMT inhibitors in Parkinson's disease

First generation COMT inhibitors (gallates, tropolone, and others) have been used for several years. Those compounds contain a catechol structure, or some related bioisosteric moiety, and are typically competitive substrates of COMT [28] (Fig. 4).

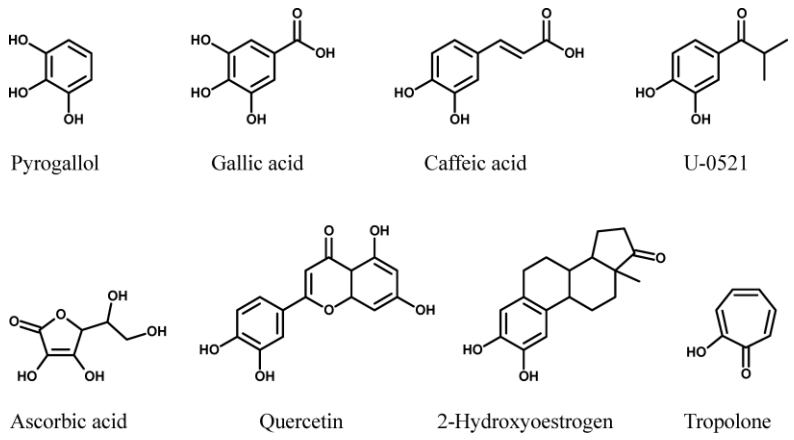

Figure 4– Representative base structures of some first generation COMT inhibitors (adapted from [28]).

Some of this early COMT inhibitors have been subjected to some limited clinical tests, but they were found to be short acting, with low in vivo efficacy, low selectivity and were rather toxic [3, 28, 32], thus showing little value as pharmacological agents [28].

Second generation COMT inhibitors constituted a new class of di-substituted catechols, obtained by substitution with electron-withdrawing groups at an *ortho* position to a hydroxyl

group of the catechol moiety. The best results were obtained with the nitro group, hence giving rise to a new class of nitrocatecholic COMT inhibitors [28], which are very potent, highly selective and orally active [3].

The concentration of the most potent nitrocatechols necessary to inhibit 50% of in vitro COMT activity was typically in the low nanomolar range, which indicates a potency three orders of magnitude higher than that of typical first generation COMT inhibitors. Also, they are kinetically characterized as reversible tight-binding inhibitors of COMT, behaving competitively with respect to the catechol substrates [28].

Second generation COMT inhibitors can be divided into three groups [3]: mainly peripherally acting compounds, broad-spectrum compounds (working in both the periphery and the brain) and atypical compounds (acting preferably in the brain).

Peripherally acting COMT inhibitors are perhaps the most interesting compounds, since they can be used as adjuncts to levodopa in PD, in order to inhibit the degradation of this compound before reaching the brain [3].

Second generation inhibitors are exemplified by nitecapone, tolcapone, entacapone and nebicapone [3, 28] (Fig. 5).

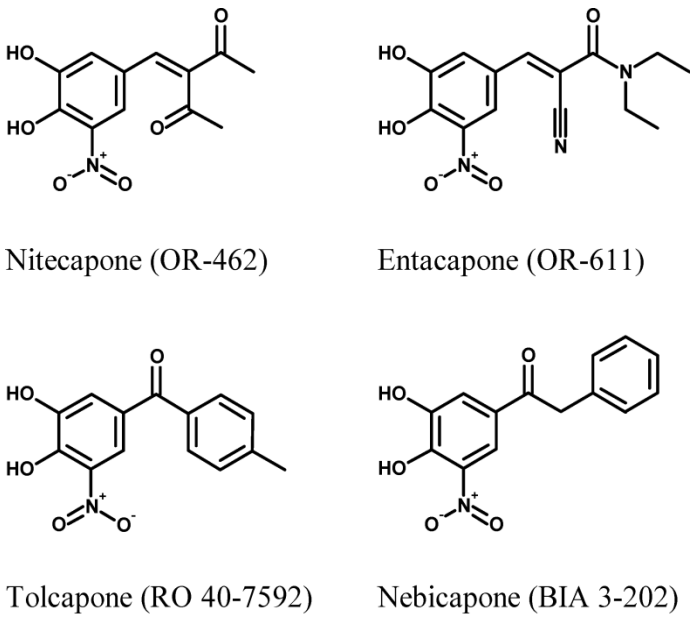

Figure 5- Chemical structures of nitecapone, tolcapone, entacapone and nebicapone (adapted from [28]).

Despite the subtlety of the differences in the mode of COMT inhibition by these inhibitors, they have very different efficacies. Entacapone is short acting and peripherally selective, and it is taken concomitantly with every dose of levodopa. It is the most widely marketed COMT inhibitor [32]. Tolcapone is more potent and longer acting than entacapone, but it is nonselective, inhibiting both cerebral and peripheral COMT. The clinical use of tolcapone is severely restricted due to its elevated hepatotoxicity risk [33]. Nebicapone has a longer duration of peripheral COMT inhibition than entacapone and more limited access to the brain than tolcapone, but due to limited clinical experience, firm conclusions concerning its safety have not yet been established [32]. Finally, nitecapone is a strictly peripheral COMT inhibitor that increases striatal levels of HVA, which reflects an increased amount of levodopa reaching and being utilized in the brain, due to inhibition of COMT in the peripheral tissues, but not in the brain [28].

Given all the problems related with first and second generation COMT inhibitors, there is a requirement for improved inhibitors to address the unmet medical needs of many PD patients [28, 32]. In an attempt to perhaps develop a third generation of COMT inhibitors, different structures have been studied, such as heterocyclic COMT inhibitors, that were found to have reduced toxicity risk and guarantee a longer duration of inhibition [32].

In the present, only two compounds are currently available, namely tolcapone, the use of which is restricted; and entacapone, a safer but less efficient compound. Nebicapone, with an efficiency between the two commercially available inhibitors and apparently safer than tolcapone, has been studied in humans. So this field still has the potential for the development of newer and different COMT inhibitors with a good and safe therapeutic profile [28].

In order to develop new COMT inhibitors, a relatively high quantity of enzymatically active COMT is needed, whether for crystallization studies needed to develop structure-based inhibitors [34], or for the *in vitro* studies needed in the first stage of drug development.

1.4 –Recombinant hSCOMT biosynthesis

The best way to obtain considerable amounts of human proteins is by recombinant technology. In the case of recombinant human SCOMT (hSCOMT), it has been produced via different expression systems, such as transfected mammalian cells [35], insect cells (via mammalian and baculovirus vectors) [36], plant cells (via a potyvirus) [37] and prokaryotic cells, such as *E. coli* [38 - 40].

Ulmanen and coworkers [35] overexpressed SCOMT and MBCOMT in mammalian (human and hamster) cell cultures, not aiming at recombinant protein production, but in order to

determine their subcellular localization. The main disadvantage of this expression system for large scale recombinant protein production is the high costs of media components necessary for cell growth [41]. Also, overexpression of recombinant proteins may exceed the cells' capacity to process synthesized polypeptides properly, leading to accumulation of proteins in anomalous localizations [35]

In 1992, Tilgmann and coworkers produced active human recombinant soluble and MBCOMT, using expression systems in transfected mammalian and recombinant baculovirus infected insect cells, obtaining a much higher amount of recombinant COMT using the baculovirus expression system [36].

More recently, plant cells infected with potato virus A (PVA) based vectors have also been used for recombinant SCOMT production, achieving high amounts of active SCOMT in plant tissues [37]. However, recombinant SCOMT obtained with this expression system had a methylation activity of only 5 to 30% of those measured from *E. coli* lysates [37].

The main sources for recombinant hSCOMT production throughout the years, however, have been *E. coli* host systems [38 - 40]. Since this expression system has an ability to grow rapidly and at high cell density on inexpensive substrates [42, 43], *E. coli* was the selected microorganism for the development of our work.

1.4.1 – Host strain and promoter selection

Escherichia coli is a gram-negative bacterium and is the most commonly used organism for heterologous protein production [41 - 45], allowing the establishment of large scale production systems due to its ability to quickly reach high cell densities in inexpensive media [42, 43, 45, 46]. Additionally, its well-known genetics with publicly available genome sequences and also the availability of a large number of cloning vectors and mutant strains [43] makes *E. coli* the microorganism of choice for recombinant protein production.

Despite all this advantages, *E. coli* presents some limitations regarding protein production issues, such as the limited ability to build disulfide bonds, the lack of an efficient secretion system (due to the complexity of its two membranes), and the inability to perform posttranslational modifications [42, 44, 47]. However, as most proteins retain their full biological activity in a non-glycosylated form, they can be effectively produced in *E. coli*, overcoming the drawbacks associated with this prokaryotic protein expression [43].

For routine protein expression, *E. coli* B and K-12 strains, along with their derivatives, are the most frequently used (Table 1), and BL21 is more suitable for protein production due to the lack of two proteases (*lon* and *ompT*) present in K12 strains [44], thus avoiding protein degradation.

One particular BL21 derivative, *E. coli* BL21 (DE3) was especially designed for the overexpression of membrane proteins, but thousands of homologous and heterologous soluble proteins were successfully expressed to high levels in *E. coli* BL21 (DE3) [44, 47]. This strain has been used for all three referred studies of COMT production in this microorganism [38], [39], [40], and so *E. coli* BL21 (DE3) was the selected strain for the development of this work.

Table 1- Some E. coli strains most frequently used for heterologous protein production and their key features (adapted from [44]).

E. coli strain	Derivation	Key features
AD494	K-12	*trxB* mutant; facilitates cytoplasmic disulfide bond formation
BL21	B834	Deficient in *lon* and *ompT* proteases
BL21 trxB	BL21	*trxB* mutant; facilitates cytoplasmic disulfide bond formation; deficient in *lon* and *ompT* proteases
BL21 CodonPlus-RIL	BL21	Enhances the expression of eukaryotic proteins that contain codons rarely used in *E. coli*: AGG, AGA, AUA, CUA; deficient in *lon* and *ompT* proteases.
BL21 CodonPlus-RP	BL21	Enhances the expression of eukaryotic proteins that contain codons rarely used in *E. coli*: AGG, AGA, CCC; deficient in *lon* and *ompT* proteases.
BLR	BL21	*recA* mutant; stabilizes tandem repeats; deficient in *lon* and *ompT* proteases
B834	B strain	Met auxotroph; ^{35}S-met labeling
C41	BL21	Mutant designed for expression of membrane proteins
C43	BL21	Double mutant designed for expression of membrane proteins
HMS174	K-12	*recA* mutant; Rif resistance
JM 83	K-12	Usable for secretion of recombinant proteins into the periplasm
Origami	K-12	*trxB/gor* mutant; greatly facilitates cytoplasmic disulfide bond formation
Origami B	BL21	*trxB/gor* mutant; greatly facilitates cytoplasmic disulfide bond formation; deficient in *lon* and *ompT* proteases
Rosetta	BL21	Enhances the expression of eukaryotic proteins that contain codons rarely used in *E. coli*: AUA, AGG, AGA, CGG, CUA, CCC, and GGA; deficient in *lon* and *ompT* proteases
Rosetta-gami	BL21	Enhances the expression of eukaryotic proteins that contain codons rarely used in *E. coli*: AUA, AGG, AGA, CGG, CUA, CCC, and GGA; deficient in *lon* and *ompT* proteases; *trxB/gor* mutant; greatly facilitates cytoplasmic disulfide bond formation

Another important step in recombinant protein production is the selection of an appropriate promoter. In order to obtain a high-level production in *E. coli*, the promoter must be strong and inducible, to enable high-level gene expression [48], resulting in the accumulation of desired protein up to 10 to 30% or more of total cell protein [47]; have a minimal level of basal transcriptional activity [47], as large-scale gene expression preferably employs cell growth to high density and minimal promoter activity, followed by induction of the promoter [43, 47]; and be able to provide a simple and cost-efficient induction [44].

Many promoter systems of *E. coli* have been developed, but only a few of them are commonly used (Table 2), with T7 RNA polymerase being the one which yields the highest level of protein expression [44].

T7 RNA polymerase is one of the most widely used expression systems. It elongates chains faster than *E. coli* RNA polymerase and it is present in the selected *E. coli* BL21 (DE3) strain chromosome, under control of a *lac* promoter derivative, meaning that it can be strongly induced by isopropyl-b-D-thiogalactopyranoside (IPTG) [44]. Typically, pET vectors are extremely popular for recombinant protein production. In this system, target genes are positioned downstream of the T7 promoter [42], and so the characteristics of T7 RNA polymerase expression system are maintained [49].

Table 2- Some *Escherichia coli* promoter systems and their specific characteristics that can be applied for heterologous protein production (adapted from [44]).

Expression system based on	Induction (range of inductor)	Level of expression	Key features
lac promoter	Addition of IPTG 0.2 mM (0.05–2.0 mM)	Low level up to middle	Weak, regulated suitable for gene products at very low intracellular level Comparatively expensive induction
trc and *tac* promoter	Addition of IPTG 0.2 mM (0.05–2.0 mM)	Moderately high	High-level, but lower than T7 system Regulated expression still possible Comparatively expensive induction High basal level
T7 RNA polymerase	Addition of IPTG 0.2 mM (0.05–2.0 mM)	Very high	Utilizes T7 RNA polymerase High-level inducible over expression T7*lac* system for tight control of induction needed for more toxic clones Relative expensive induction Basal level depends on used strain (pLys)
Phage promoter p_L	Shifting the temperature from 30 to 42 °C (45 °C)	Moderately high	Temperature-sensitive host required Less likelihood of "leaky" uninduced expression Basal level, high basal level by temperatures below 30 °C No inducer
tetA promoter/operator	Anhydrotetracycline 200µg/l	Variable from middle to high level	Tight regulation Independent on metabolic state Independent on *E. coli* strain Relative inexpensive inducer Low basal level
araBAD promoter (P_{BAD})	Addition of L-arabinose 0.2 % (0.001–1.0 %)	Variable from low to high level	Can fine-tune expression levels in a dose-dependent manner Tight regulation possible Low basal level Inexpensive inducer
rhaP$_{BAD}$ promoter	L-rhamnose 0.2 %	Variable from low to high level	Tight regulation Low basal activity Relative expensive inducer

As mentioned above, IPTG is the inducer of choice for the selected expression system. Although IPTG's cost is often argued to limit the usefulness of IPTG-inducible promoters [42], they are powerful and widely used for basic research [47], and cost-related problems are rarely applicable for high added value products [42]. Another problem associated with IPTG is its toxicity, and so, the minimum amounts needed to achieve full induction should be used [42].

1.4.2 – Fermentation strategies, conditions and monitoring

It is known that *E. coli* is able to grow in salt-based chemically defined media, as long as an organic carbon source and a nitrogen source are provided, as well as in complex organic media [40]. However, it has been proved that it's not enough to meet bacterial nutritional requirements to ensure that they continue to grow [46], in fact, several aspects affect bacterial growth, such as temperature, pH, agitation rate (directly related to oxygen transfer) and the presence of toxic or inhibitory compounds in the medium [45, 46]. For this particular strain, a semi defined medium has already been described, and in our research group, hSCOMT has already been produced via a fed-batch process [40].

Passarinha and coworkers [40] studied the best growth conditions for the production of hSCOMT in this *E. coli* expression system, firstly in shake flask experiments. The semidefined medium (Table 3) was tested with different carbon sources (glucose and glycerol) concentrations (Fig. 6).

Table 3 – Semidefined medium composition (adapted from [40]).

Component	Concentration
Na_2HPO_4	5.50 g/l
NaCl	0.50 g/l
Citric acid monohydrated	1.64 g/l
Potassium citrate	2.00 g/l
Sodium citrate	0.67 g/l
Triptone	20 g/l
Glycerol	30 g/l
$MgSO_4 \cdot 7H_2O$	1.21 g/l
Carbenicillin	50 µg/ml
Trace elements	1.5 ml
Trace elements composition	
$FeCl_3 \cdot 6H_2O$	27 g/l
$ZnCl_2$	2 g/l
$CoCl_2 \cdot 6H_2O$	2 g/l
$Na_2MoO_4 \cdot 2H_2O$	2 g/l
$CaCl_2 \cdot 2H_2O$	1 g/l
$CuSO_4$	1.2 g/l
H_3BO_3	0.5 g/l

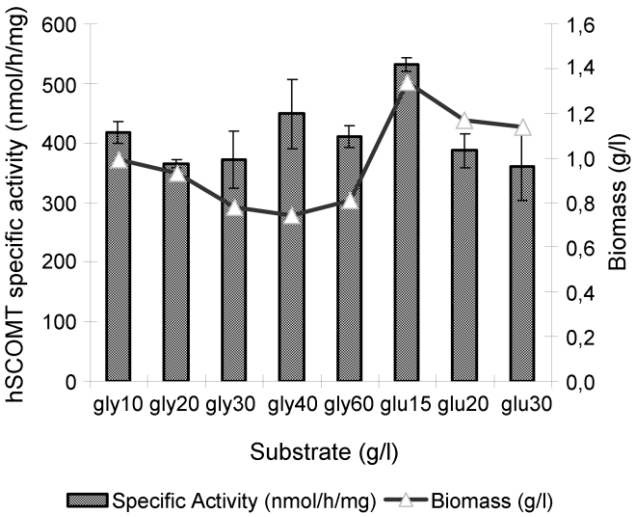

Figure 6 – Comparative studies of different carbon sources (gly, glycerol; glu, glucose) and concentrations in terms of hSCOMT specific activity (nmol/h/mg) and biomass (g/L) yields (adapted from [40]).

Their results showed that higher glucose concentrations inhibit cell growth, leading to lower hSCOMT specific activity. The best results in terms of cell growth and enzymatic activity were achieved with a low (15 g/L) concentration of glucose, but this concentration can promote several adverse effects during scale-up. Glycerol concentration did not show this effect, and the best performance at this scale was obtained with 10 g/L of glycerol in the culture medium [40].

Subsequently, fed-batch fermentations were performed, and a feeding strategy of exponential followed by constant feeding was found to provide the best results in terms of biomass (10 g dry cell weight (dcw)/L in 19h), with a growth rate of 0.3 h^{-1} (Fig. 7). These results were then validated, achieving a final volumetric accumulation after 3 h of induction around 580 U/L.

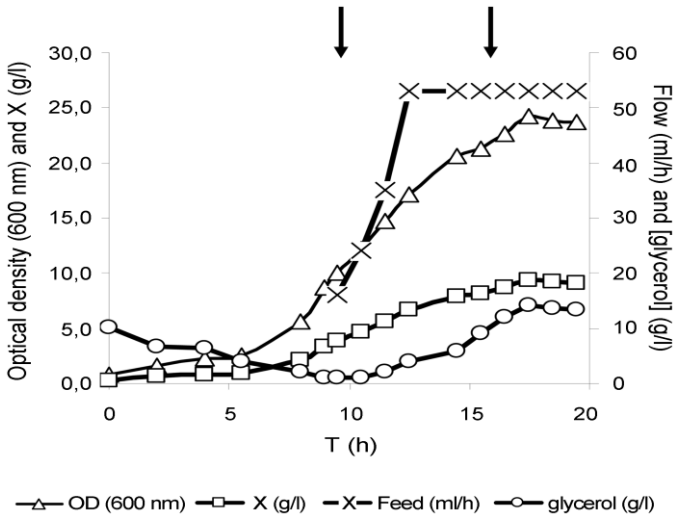

Figure 7 – Behaviour of cultivation parameters during fed-batch procedure. The starting of the feeding and induction are indicated by the left and right arrows, respectively. OD, optical density [dcw (g/L) = 0,3863 s OD]; X, biomass concentration (g/L) (adapted from [40]).

In a different study, Silva and coworkers [39] optimized the production of hSCOMT using the same *E. coli* expression system but with a different approach based on artificial neural networks, in shake flask experiments. A method combining central composite design and artificial neural networks was applied to the above mentioned semidefined medium and a complex medium (SOB medium), to optimize the fermentation conditions for the production of hSCOMT. Temperature, pH and stirring rate were selected as input variables, with total hSCOMT activity being the response variable, and also monitoring biomass concentration levels. The optimization procedure adopted in this work lead to a maximum hSCOMT activity of 183.73 nmol/h onto a semi-defined medium at 40°C, pH 6.5 and stirring rate of 351 rpm [39]. The experimental strategy and validation presented left new perspectives for further trials.

Apart from the optimization of growth conditions mentioned above, to achieve high quantities of recombinant protein production, large-scale culture processes have to be applied, mostly based on fed-batch mode cultures [45, 46, 50].

A fed-batch culture is generally started with an inoculum growing at the maximum specific growth rate that can be sustained using the nutrients initially present in a bioreactor, followed by the imposition of a specific regime of nutrient feed until fermentation is complete [45]. These methods are based on mathematical models that describe growth patterns and the expected demand for nutrients [46].

The method of nutrient feeding is critical to the success of a fermentation process, as it affects both the maximum attainable cell concentration and productivity. Regarding the pattern of nutrient addition, three main types of pre-determined feeding profiles can be considered: constant, exponential and stepwise feeds [45].

In constant feeding, nutrients are fed into the bioreactor at a predetermined rate that does not change during the process. Due to the increase in culture volume and cell concentration, the specific growth rate continuously decreases [45]. In stepwise (or gradual) increasing feeding, nutrients are fed at ever increasing rates. It can enhance growth by supplying more nutrients at higher cell concentrations. Cell growth can be exponential during the entire culture period if the feed rate is increased in proportion to cell growth [45].

Exponential feeding allows cells to grow at predetermined specific growth rates, usually between 0.1 and 0.3 h^{-1}, that can be set to fall below the maximum specific growth rate and also avoid acetate formation (a growth limiting by-product for *E. coli*) [45, 51].

Typically, the feeding rate can be calculated using a standard equation [45, 46] (1).

$$Ms(t) = F(t)Sf(t) = \left(\frac{\mu}{YX/S} + m\right) X(t)V(t) = \left(\frac{\mu}{YX/S} + m\right) X(t0)V(t0)\exp[\mu(t - t0)] \quad (1)$$

M – mass-flow rate of the carbon source (g/h)
F – feed flow-rate (h^{-1})
S_f – substrate concentration in the feeding solution (g/L)
μ - specific growth rate (h^{-1})
$Y_{X/S}$ – cell yield on carbon substrate, specific for each strain (g dcw/g substrate)
m – specific maintenance coefficient (g/(g dcw h)
X – cell concentration (g/L dcw)
V – culture volume (L)
t_0 – time of feeding start (h)
t – process time (h)

Another feeding approach that can be used is the direct and indirect feedback control systems for the controlled addition of nutrients. Indirect control is based on online monitoring of parameters such as pH, dissolved oxygen, CO_2 evolution rate and cell concentration. Direct feedback is based on monitoring the concentration of the major carbon substrate. [45, 46]

Besides all the fermentation conditions and strategies mentioned above, there are important additional factors that can interfere with cell growth and, consequently, with protein production.

One of the most important factors to monitor is cell physiology, a critical parameter in recombinant fermentations, since alterations in cell physiological state may reflect alterations in the host cell metabolism [52].

Bacteria are relatively difficult to analyze by flow cytometry, the best tool to assess cell viability, mostly due to their reduced size, but technical advances in instrumentation and methodology are leading to an increased popularity of flow cytometry and its range of applications in biotechnological processes [53].

One of the most used parameters to determine cell viability is membrane potential, which is considered a measure of the health of microorganisms, because only live cells are able to maintain its membrane potential. Membrane depolarization means a decrease in cell activity, but it does not imply cell death, it means that the membrane is structurally damaged and ions can go across it freely [54].

Membrane potential measurements are carried out by means of lipophilic dyes which go through the cell membrane and accumulate inside the cell when the membrane is depolarized according to its charge. Oxonols, such as BOX (Bis-(1,3-dibutylbarbituric acid)trimethine oxonol) are anionic and lipophilic, accumulating inside non-viable cells [54].

The evaluation of membrane integrity is the most definitive proof of cell viability. Cells showing intact membranes are impermeable to multiple charged dyes, the most common being propidium iodide (PI), but if cells loose membrane integrity, these dyes enter into the cells and emit fluorescence upon binding to nucleic acids [54]. Cells with damaged or compromised membranes cannot maintain or generate the electrochemical gradient and hence the membrane potential, and if a PI/BOX dual staining is used, these cells will emit fluorescence corresponding to both of these dies [53, 54].

Chapter 2 - Materials and Methods

2.1 - Materials

Ultrapure reagent-grade water was obtained from a Mili-Q system (MIlipore/Waters). Carbenicillin disodium salt, calcium chloride dihydrate, magnesium sulfate heptahydrate, lysozyme, cobalt(II) chloride hexahydrate, dithiotreitol (DTT), SAM chloride salt, DNase, epinephrine (bitartrate salt), disodium ethylenediamine tetraacetic acid (EDTA), sodium octyl sulphate (OSA), bovine serum albumin (BSA), LB-Agar, IPTG, tryptone, glycerol and PI were obtained from Sigma Chemical Co. (St Louis, MO, USA). Potassium chloride, sodium chloride, boric acid were supplied by Fluka (Buchs, Switzerland). Sodium phosphate dibasic and potassium dihydrogen phosphate monobasic were obtained from Panreac (Barcelona, Spain). Bis-(1,3-dibutylbarbituric acid)trimethine oxonol (BOX) was obtained from Invitrogen Corporation (Carlsbad, CA, USA). All other chemicals were of analytical grade and used without further purification.

2.2 – Methods

2.2.1 – Expression vector and bacterial strain

The Champion pET101 Directional TOPO expression kit (Invitrogen Corporation, Carlsbad, CA, USA) was used for the expression of hSCOMT on *E. coli* BL21(DE3) strain gently provided by Bial (São Mamede do Coronado, Portugal).

2.2.2 - *Escherichia coli* pre-cultivation, batch and fed-batch conditions

In this study, except for tryptone and glycerol levels, all media components for the semi-defined medium were kept constant (5.5 g/L Na_2HPO_4, 0.5 g/L NaCl, 1.64 g/L citric acid monohydrate, 2 g/L potassium citrate, 1.21 g/L $MgSO_2 \cdot 7H_2O$, 50 µg/mL carbenicillin and 1.5 mL/L trace elements solution) for the pre-cultivations batch and batch phase of fed-batch experiments. The trace elements solution consisted of 27 g/L $FeCl_3 \cdot 6H_2O$, 2 g/L $ZnCl_2$, 2 g/L $CoCl_2 \cdot 6H_2O$, 2 g/L $Na_2MoO_4 \cdot 2H_2O$, 1 g/L $CaCl_2 \cdot 2H_2O$, 1.2 g/L $CuSO_4$ and 0.5 g/L H_3BO_4, prepared in 1.2 M HCl. The LB Agar plates with 50 µg/mL carbenicillin were inoculated from a cell bank aliquot and grown overnight at 37°C. From the plate, a single colony was inoculated in a 500 mL shake flask containing 125 mL of semi-defined medium, and grown at 37°C and

250 rpm until an OD_{600} (optical density at 600 nm)of approximately 2.6 was reached. Batch and fed-batch processes were carried out in 750 mL bench-top parallel mini-bioreactors (Infors HT, Switzerland) with 250 mL of the semi-defined medium. The bioreactors were inoculated from the pre-cultivation to obtain a starting OD_{600} of approximately 0.2. The temperature and pH were kept constant throughout the batch and fed-batch phases at 40°C and 6.5 (previously optimized by our research group [39]) respectively, with the pH value controlled by the automatic addition of 0.75 M H_2SO_4 and 0.75 M NaOH through two peristaltic pumps. The pO_2 (dissolved oxygen percentage) was controlled by a two-level cascade of stirring (between 250 and 900 rpm) and air flow (between 0.2 and 2).

The feeds consisted of different concentrations of tryptone and glycerol dissolved in deionized water and the different feeding profiles tested were maintained by the automated peristaltic pumps controlled by IRIS software (Infors HT, Switzerland).

2.2.3 – Flow cytometry assays

In order to assess cells' viability during the fermentation experiments, samples were retrieved at specific times and treated for the flow cytometry assays. The OD_{600} of the samples was measured and a dilution with PBS (8 g/L NaCl, 0.2 g/L KH_2PO_4, 1.5 g/L Na_2HPO_4 and 0.2 g/L KCl) was prepared to obtain a final OD_{600} of 0.2 (approximately $1x10^8$ cells/mL and further diluted in PBS with 4mM NaEDTA to a cell concentration of about $1x10^6$ cells/mL). To this cell suspension, the appropriate volumes of PI and BOX were added in order to attain final concentrations of 10 and 2.5 µg/mL, respectively. The samples were incubated for 15 min at room temperature in the dark, centrifuged for 5 min at 5000 rpm and resuspended in PBS prior to analysis in the CyAn ADP flow cytometer (Beckman Coulter Inc., California, United States). Acquisition was performed with Summit Software (Beckman Coulter Inc., Brea, CA). The acquisition was based on light scatter and fluorescence signals resulting from 25 mW solid state laser illumination at 488 nm. Fluorescence signals were collected by FL1 (530/40 nm, BOX) and FL4 (680/30 nm, PI) bandpass filters. Light scattering, BOX and PI fluorescence measurements were acquired logarithmically. Threshold was set on SSC to exclude noise, other particles and debris. Cells were gated according to light scatter parameters. Sample acquisition was operated at flow rate of no more than 300 events per second and a total of 5000 events were acquired for each sample.

2.2.4 – Glycerol assess

For glycerol assessment, samples were also retrieved at specific times and centrifuged at 4°C and 16000g for 5 minutes. The resulting supernatant was then filtered through a 0.22 µm filter for HPLC (high performance liquid chromatography) injection.

Quantification was carried out using an Agilent 1290 Infinity LC HPLC system (Waldbronn, Germany) coupled with a Refractive Index Detector (RID) (Agilent 1260 Infinity). Compound separation was done using a Hi-Plex H ion-exchange analytical column (Agilent, Santa Clara, CA, USA) with a 7.7 x 300 mm and 8 µm pore size. The mobile phase consisted of a 2.5 nM H_2SO_4 solution prepared with ultrapure water, filtered through a 0.2 µm pore membrane and degassed for 15 min before use. Flow rate was set to 0.6 mL/min and column temperature was set to 65°C.

2.2.5 – Cell lysis

Intracellular SCOMT was obtained via a combined lysis process. Typically, 2 mL of samples from fermentations were centrifuged at 4°C and 16000g for 5 minutes, ressuspended with 500 µL of a standard buffer buffer (150 mM NaCl, 10 mM DTT, 50 mM Tris, 5 µg/mL leupeptin and 0.7 µg/mL pepstatin), transferred to lysis tubes and kept on ice. Subsequently, in order to perform the enzymatic lysis, 100 µL of 10 mg/mL lysozyme solution were then added to each tube and incubated at room temperature for 15 minutes. The disruption step continued by a freeze-thaw method, with the tubes submerged in liquid nitrogen until frozen and transferred to a 42°C bath for thawing. This process was repeated for 6 times to ensure maximum lysis efficiency. After this procedure, 50 µL of 1 mg/mL DNase solution were then added to each tube and the samples were centrifuged for 20 minutes at 4°C and 16000g. The resulting supernatant, containing the solubilized SCOMT, was then used as sample for the activity and protein quantitation assays.

2.2.6 – Protein assessment assay

The protein quantitation assay was carried out using a Pierce BCA Protein Assay kit (Thermo Scientific, USA) on a 96 well plate, and a specific volume of working reagent (WR) was prepared from solutions A and B from the kit according to the number of existing samples and blanks as follows:

$$V\ of\ WR\ (\mu L) = [(number\ of\ samples + number\ of\ blanks) \times 3] \times 200 \quad (2)$$

Given this volume, the proportion of both solutions was calculated based on equations 3 and 4:

$$\frac{V\ of\ WR}{50} = V\ sol.B\ (\mu L)\ (3)$$

$$V\ sol.A\ (\mu L) = V\ of\ WR - V\ sol.B\ (4)$$

Then, 25 µL of each sample or blank (in triplicates) and 200 µL of WR were added to each well and homogenized. The plate was then incubated at 37°C for 30 min, after which the absorbance at 570 nm was measured and the values applied to a previously calculated calibration curve.

For the calibration curves, several solutions of different BSA concentrations (25, 125, 250, 500, 750, 1000, 1500 and 2000 µg/mL) were prepared in triplicates using a standard buffer (150 mM NaCl, 10 mM DTT, 50 mM Tris, 5 µg/mL leupeptin and 0.7 µg/mL pepstatin), 1/100 diluted. BSA solutions and 1/100 diluted standard buffer (working as blank) were subjected to the quantitation assay as mentioned above, and their absorbance measured at 570 and 595 nm. The results of the three replicates for each BSA concentration and the blank were averaged and two calibration curves were plotted, on for each wave length (Fig. 8 and 9).

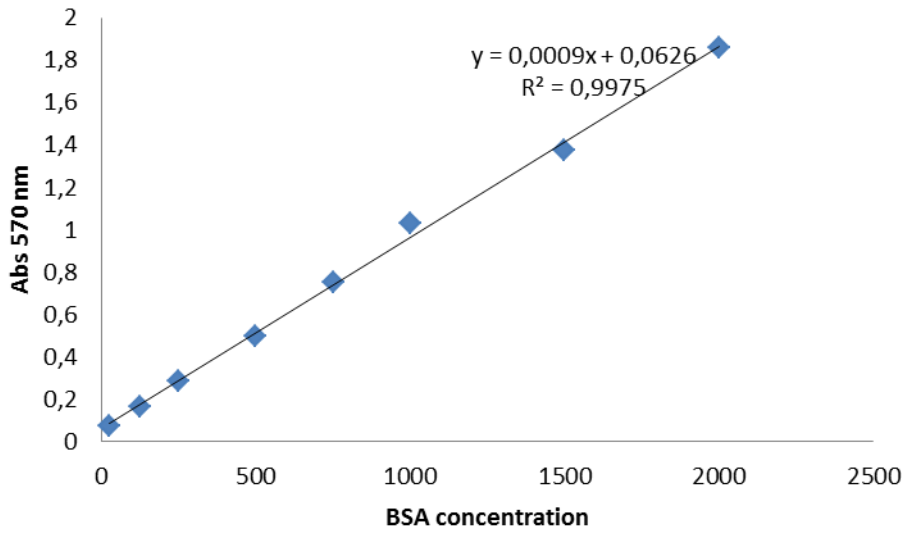

Figure 8 – Calibration curve for BSA solutions absorbance at 570 nm.

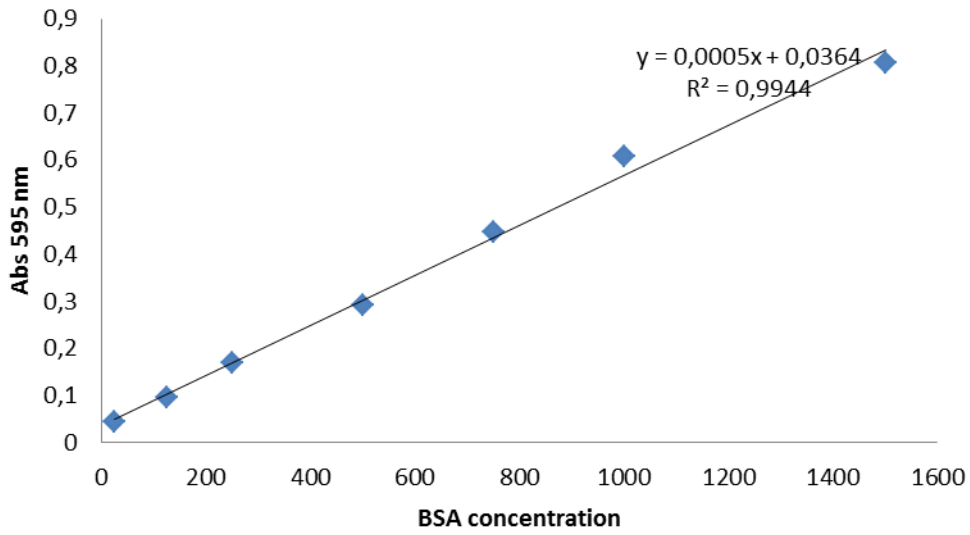

Figure 9 – Calibration curve for BSA solutions absorbance at 595 nm.

Given the plots, the chosen wave-length for the assay was 570 nm, as it presented the best results (a R^2 of 0.9975) compared to the 595 nm curve, and its equation was used to assess the quantity of total protein in the samples.

2.2.7 – Enzymatic activity assay

The enzyme activity was measured via the quantity of metanephrine produced as a result of the reaction between hSCOMT and the substrate epinephrine.

The samples for this assay were prepared to a final volume of 250 µL by diluting a certain amount of the resulting supernatant of the lysis process in standard buffer (described above) in order to obtain the same amount of protein on each sample (150 µg/mL), based on the quantitation assays results (5).

$$150\ \mu g/mL \times 250\ \mu L = [protein\ in\ sample] \times Vsupernatant \quad (5)$$

The experiments were carried out in refrigerated, foil covered test tubes, adding 250 µL of the diluted sample and 200 µL of incubation solution (0.272 mg/mL SAM, 1 µL/ML $MgCl_2$ (0.2 M), 40 µL/mL ethylene glycol tetraacetic acid (EGTA) (50 mM) and 959 µL/mL phosphate buffer) and incubating them for 5 min in a water bath at 37°C and 83 RPM. After 5 min, 50 µL of epinephrine solution (3.331 µg/mL, dissolved in incubation solution) were added, in order to let the enzymatic reaction to occur for 10 minutes. After 10 minutes, the reaction was stopped by transferring the tubes to ice and adding 100 µL of perchloric acid (2 M). The tubes were then kept at 4°C for 1 hour, after which the resulting samples were transferred to

eppendorfs and centrifuged for 10 min at 4°C and 6000 RPM. The samples were the filtered through a 0.22 µm pore size filter to remove precipitated biomaterial and injected to an HPLC system.

The HPLC injections were performed using a HPLC model Agilent 1260 system (Agilent, Santa Clara, CA, USA) equipped with an autosampler and quaternary pump coupled to an ESA Coulochem III (Milford, MA, USA) coulometric detector. Chromatographic separation was achieved on an analytical column Zorbax 300SB C_{18} reverse phase analytical column (250 x 4.6 mm i.d. 5 µm) (Agilent, Santa Clara, CA, USA). The mobile phase (0.1 M sodium dihydrogen phosphate, 0.024M citric acid monohydrate, 0.5 mM OSA and 9% acetonitrile, v/v), pH 2.9, was filtered under vacuum (0.2 µm hydrophilic polypropylene filter), degassed in ultrasonic bath before use. Column effluent was monitored with an electrochemical detector by a coulometric mode, which was equipped with a 5011 high sensitivity dual electrode analytical cell (electrodes I and II) using a procedure of oxidation/reduction (analytical cell #1: +410 mV; analytical cell #2: -350 mV). The flow rate applied was 1 mL/min. Column temperature was optimized to 30ºC. The chromatograms were obtained by monitoring the reduction signal of the working electrode II.

Chapter 3 - Results and Discussion

In recent years, several attempts have been performed to obtain a large quantity of enzymatically active and pure hSCOMT. The first step to achieve this aim is to develop an adequate up-stream strategy, which means high levels of recombinant enzymatic production in an active form, in order to facilitate the subsequent purification steps. One of the most effective ways of enhancing recombinant protein production is the application of a fed-batch process, which highly increases cell density and, subsequently, protein production. However, a fed-batch process has its particularities, and it must be finely tuned to obtain the desired results.

In this work, a fed-batch bioprocess based on previously optimized culture conditions [39] was developed, via an up-scaling of hSCOMT production. Initially, several batch fermentations were carried out, in order to establish and optimize culture conditions, batch phase and bioreactor operation for the fed-batch fermentations. After this stage, a series of fed-batch fermentations with different feeding strategies were tested in order to obtain the maximum biomass production.

3.1 – Batch fermentations

As mentioned above, Silva and coworkers [39] optimized three physical culture conditions for the production of hSCOMT in shake flasks, namely temperature (40° C), pH (6.5) and stirring rate (351 rpm), and this was the starting point for the strategy described in the present work.

Since the optimization was performed in bench-top parallel mini-bioreactors, and at this scale the stirring rate was not kept constant throughout the fermentations, the optimized 351 rpm stirring rate wasn't applicable. As the agitation speed is associated with the dissolved oxygen concentration, the dissolved oxygen concentration was the parameter to optimize in this first step of our work, in order to assess the best value to be used in subsequent experiments, while temperature and pH values were kept constant in all of the experiments carried out through the whole work. Dissolved oxygen concentration in culture media, maintained by a cascade of agitation and airflow, in which agitation is constantly increased from 250 up to 900 rpm, followed by a constant increase of air flow from 0.2 to 2 (starting when maximum agitation is reached).

Dissolved oxygen concentration is one of the most difficult variables to reproduce, due to the combination of low solubility in water (even lower at higher temperatures) and, when cell density increases, the high nutritional demand [55] demands for pure oxygen supplementation to the culture media.

Since our studies were carried out at relatively high temperature (40°C), oxygen solubility is consequently lower, and so this is in fact an important parameter to establish in the first stages of a bioprocess.

Firstly, two batches were performed at 30% dissolved oxygen [40] to determine the typical growth curve under these conditions (Fig. 10). The medium composition was the previously described in section 2.2.2 of the Materials and Methods section, with a concentration of glycerol and tryptone of 30 and 20 g/L, respectively.

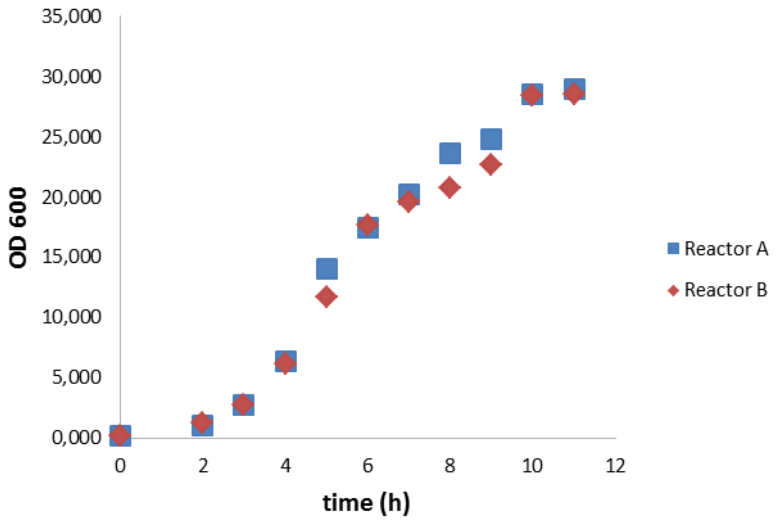

Figure 10 - Growth curve of *E. coli* in a batch process: 40°C, 30% dissolved oxygen, pH 6.5.

The growth curve presented in Fig. 10 showed that the stationary phase is reached after approximately 8 hours of fermentation. Under these conditions the maximum OD attained is of about 28.

The maximum obtained OD is surprisingly higher than the values previously obtained in our research group [40] for fed-batch fermentations applied to the same strain, medium and dissolved oxygen concentration.

In fact, just by applying the physical parameters optimized by Silva and coworkers [39] to a bioreactor scale, maximum OD values reached were promising, since no further optimization was until that point carried out.

Subsequently, the next step was to test three standard set-points for dissolved oxygen concentrations (20 and 40%, as well as the already used 30%), accomplishing this strategy by recombinant COMT induction

When using recombinant *E. coli*, growth and production phases can be separated, taking advantage of regulated promoters to achieve high cell densities in the first phase (while the promoter is "off"), and then high rates of heterologous protein production in the second phase (following induction) [56]. Given this information, cell culture should be grown until the beginning of the stationary phase, so that high cell densities are achieved prior to induction.

So, the three different dissolved oxygen set-points (20%, 30% and 40%) were tested in duplicates (Fig.11, 12 and 13). Fermentations were stopped four hours after induction. For activity assays, samples were retrieved at the end of the fermentation.

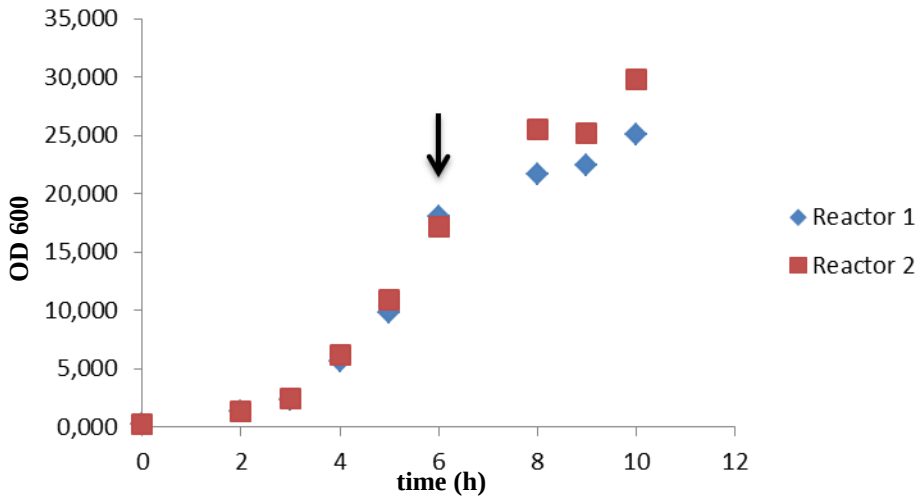

Figure 11 - Growth curve of *E. coli* in a batch process with 20% dissolved oxygen. Arrow indicates the induction time.

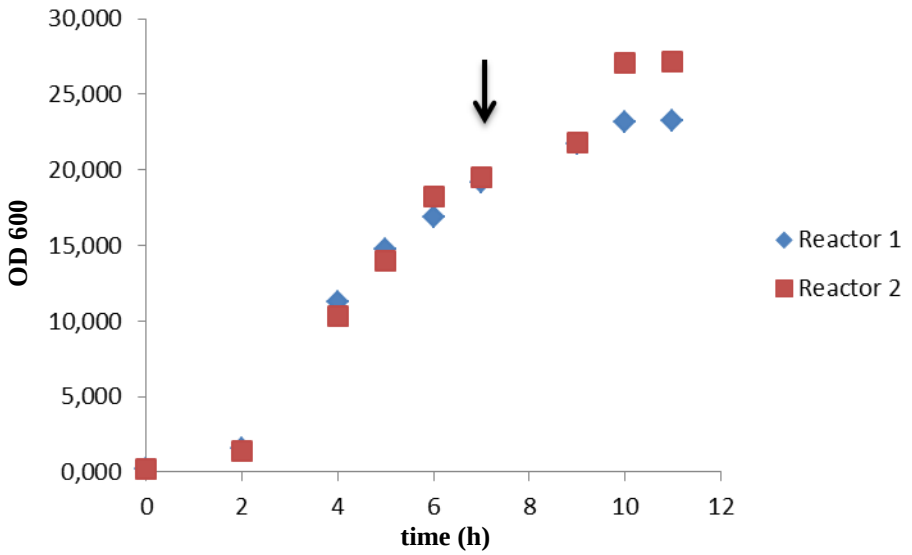

Figure 12- Growth curve of *E. coli* in a batch process with 30% dissolved oxygen. Arrow indicates the induction time.

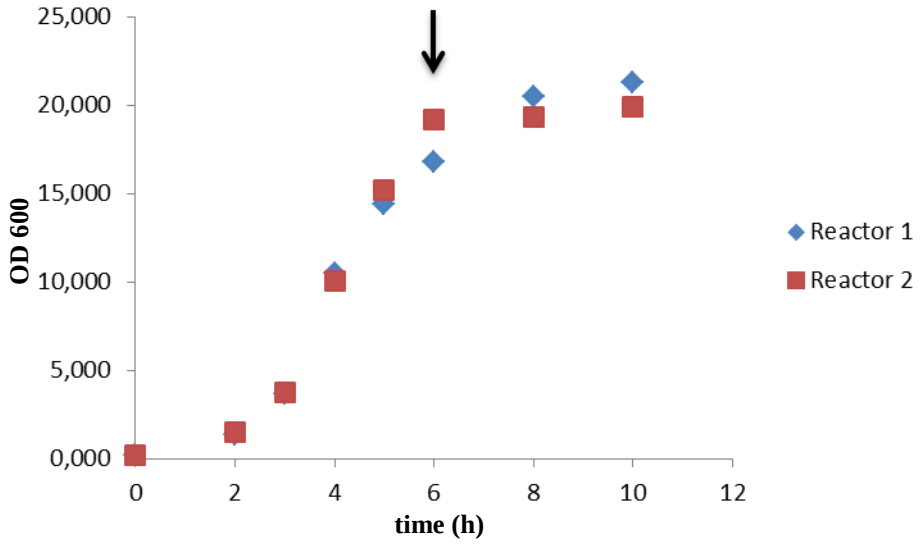

Figure 13 - Growth curve of *E. coli* in a batch process with 40% dissolved oxygen. Arrow indicates the induction time.

Based on the maximum OD reached, these results showed that the batch at 20% oxygen gives better results than 30% and 40%. This may not correspond to the expected results as higher percentages of dissolved oxygen should allow increased cell growth. However, the maintenance of the set value of dissolved oxygen is not possible throughout the whole batch process using agitation and airflow cascade, indicating that oxygen supplementation might be required to conserve such dissolved oxygen levels. In fact, at advanced stages of fermentation, even the highest values of agitation and aeration cannot compensate oxygen consumption by the bacteria, and oxygen percentage in the medium will decrease. So, if the predetermined percentage of dissolved oxygen is higher, that point will be reached earlier in

the fermentation, and cells will also reach a phase of oxygen depletion earlier in the process, which may impair cell growth and protein biosynthesis.

Then, two more assays at 20% dissolved oxygen were performed, with samples for enzymatic assay being withdrawn every hour after induction, to verify whether there was a peak of activity during this four hour period. We concluded that the best time to assess enzymatic activity was, in fact, four hours after induction, due to the fact that those times corresponded to the highest values of specific COMT activity values (316.16 and 237.20 nmol/h/mg for each assay, respectively), what is in agreement with previously obtained values [39], [40].

3.1.1 – Definition of batch phase composition

The next step in this study was to define the carbon and nitrogen sources concentrations in the batch phase for the fed-batch process, in order to reduce the time of the batch phase, and also to increase cell density at the end of the batch phase. It is important to reduce batch and fed-batch times so that nutrients/oxygen depletion is avoided, or at least minimized.

To achieve this aim, the concentration of carbon and nitrogen sources (glycerol and tryptone, respectively) were varied, resulting in three formulations (Table 4).

Table 4 - Glycerol and tryptone concentrations for the three formulations.

	1st	2nd	3rd
Glycerol (g/L)	20	10	20
Tryptone (g/L)	20	15	30

Regarding carbon source, it is known that, when compared to glucose, glycerol could be a better carbon source choice due to the yield of reduced acetate levels and low growth inhibition at high concentrations [40, 42, 45, 54]. From previous work in our group [40] and at least another study [58], glycerol can yield higher protein production levels in *E. coli*. Lower concentrations of glycerol (10 to 20 g/L) were proven to be preferable for highest hSCOMT specific activity [40], and so these were the chosen concentrations for this step of the work.

Tryptone concentration variations were kept around the 20 g/L concentration present in the semi defined medium, because it was previously optimized, and so there was none specific require to introduce markedly different concentrations.

For these assays, glycerol concentration in the supernatant was measured every two hours until stationary phase was reached, and during the stationary phase samples were retrieved every hour to assess glycerol consumption throughout fermentation.

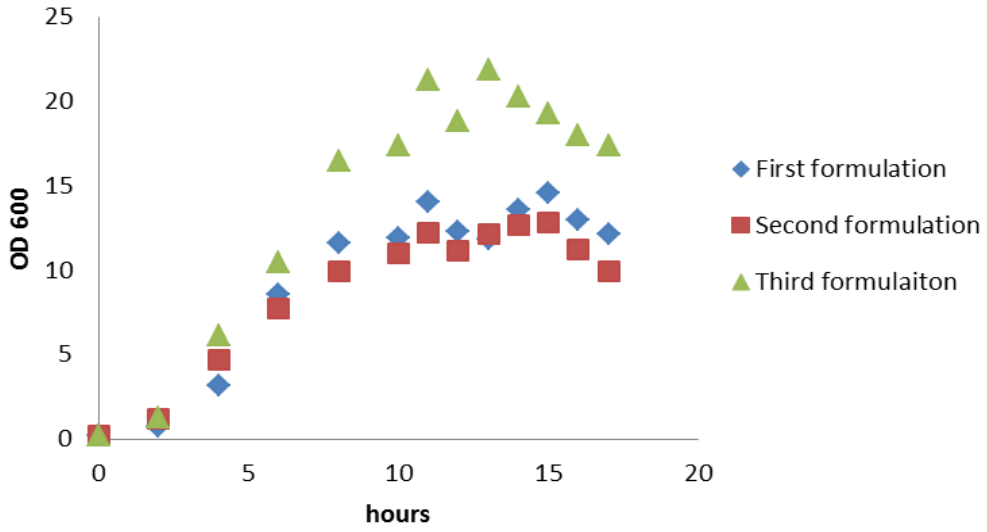

Figure 14 - Growth curves of the assays corresponding to the three formulations. 1st formulation, 20 g/L tryptone and glycerol; 2nd formulation, 10 g/L glycerol and 15 g/L tryptone; 3rd formulation, 20 g/L glycerol, 30 g/L tryptone.

From Figure 14, it appears that tryptone greatly influences cell growth, for the fermentation with the higher tryptone concentration (3rd formulation) yielded higher optical densities, whereas the fermentation with the lowest tryptone concentration (2nd formulation) showed a decreased cell density when compared with the other two results.

Glycerol does not seem to have such a great impact in cell growth in the low concentrations used in these experiments, since the two formulations with different glycerol concentrations (1st and 2nd) allowed the obtention of similar growth profiles and cell densities, which meets the results previously obtained by our research group [40].

Since the main aim of these experiments was to reduce the batch phase time, the selected formulation was the one with both glycerol and tryptone at a concentration of 20 g/L, formulation number one, due to the fact that nutrient exhaustion occurred at a lower fermentation time.

At the end of these experiments, two fermentation conditions were already selected for application in the fed-batch process, namely a dissolved oxygen concentration of 20% and glucose and tryptone concentration of 20 g/L in the batch phase.

3.2 – Growth rate and time of fed-batch initiation

The last parameters to be assessed before initiating the fed-batch processes were the growth rate of this strain under these conditions, and the time at which to initiate the feeding process.

Regarding to the growth rate, μ (h^{-1}), it can be calculated via equation (6):

$$\mu = \frac{(\ln(Nt) - \ln(N0))}{t} \quad (6)$$

where N_t is the OD_{600} (or dry cell weight, DCW) at t hours, N_0 is the OD_{600} (or dcw) at the beginning of the fermentation, and t is the time at which the culture reaches the end of the exponential phase (in hours).

So, in our case, the growth rates obtained for each formulations (Figure 14) were as depicted in table 5.

Table 5 - Growth rates for the three formulations.

μ (h^{-1})		
1st	2nd	3rd
0,51	0,49	0,55

The obtained growth rates for each glycerol/tryptone combination (table 5) were very similar and consistent with previously estimated values in our research group [40] (about 0.50 μ (h^{-1}) for a glycerol concentration of 10 g/L).

A fed-batch culture uses an inoculum growing at the maximum specific growth rate that can be sustained using the nutrients initially present in the bioreactor, and for exponential feeding it is usually maintained between 0.1 and 0.3 h^{-1} to avoid acetate formation [45] and to ensure nutrient limitation. Given this, it is important to know exactly when the carbon source is completely depleted, because the fed-batch process should be initiated at that stage (Table 6).

In this study, only the carbon source (glycerol) was evaluated, due to its easier off-line monitorization when compared to tryptone, a complex substrate.

Table 6 – Glycerol monitoring over time for the three formulations tested in subsection 3.1.1. I, II and II correspond to the 1st (20 g/L glycerol), 2nd (10 g/L glycerol) and 3rd formulations (20 g/L glycerol), respectively.

Sample	Glycerol (g/L)	Sample	Glycerol (g/L)	Sample	Glycerol (g/L)
I 4h	16,65014814	II 4h	13,06535107	III 4h	16,57738479
I 6h	9,780387485	II 6h	9,950169285	III 6h	15,28437696
I 8h	6,34044112	II 8h	5,640056457	III 8h	10,59870514
I 10h	2,025428787	II 10h	2,402548681	III 10h	5,093755868
I 11h	0,113179642	II 11h	0,627927111	III 11h	1,842239374
I 12h	0,125978265	II 12h	0,082363616	III 12h	0,143234925

Results are consistent with the initial glycerol concentrations in each fermentation. The 1st and 3rd fermentations were started at an initial glycerol concentration of 20 g/L, and the 2nd at 10 g/L, and after four hours of fermentation, only a small amount of that initial glycerol was consumed. The 2nd fermentation shows a contradictory result, as the glycerol concentration after four hours is higher than the initial 10g/L. This was probably due to operator error. As the cell culture exponentially grows, so does glycerol consumption, and after 11 hours of fermentation almost all of the glycerol present in the culture is consumed (except for the 3rd replicate, which still shows a glycerol concentration of about 1.8 g/L).

So, as the fed-batch should only be initiated when all the substrate is consumed, the selected time for fed-batch initiation was at 10.5 hours of fermentation.

3.3 – Fed-batch fermentations

Given all the previous assays, the fed-batch fermentations were initiated with a glycerol and tryptone concentrations of 20 g/L in the batch phase, dissolved oxygen rate was set to 20% and feeding was initiated at 10.5 hours of batch fermentation.

For the preliminary fed-batch studies, three constant feeding rates and three exponential rates were developed. The chosen rates for the constant feeding were 1, 3 and 6 g glycerol/L/h and 0.1; 0.2 and 0.3 h^{-1} for exponential feeding. These feeding profiles were chosen based on previously described feeding profiles [40], on the typical growth rates for

exponential feeding [45], and on the maximum specific growth rates obtained for the batch fermentations, since the growth rates selected for the feeding should be lower than the maximum value obtained, in order to guarantee complete glycerol consumption.

3.3.1 – Constant feeding profiles

In a constant feeding strategy, a predetermined constant rate of glycerol is fed to the reactor [45]. To achieve the desired rates (1, 3 and 6 g glycerol/L/h), several feed mediums with different glycerol concentrations were prepared (Table 7).

For example, for the 1 g/L/h feeding rate, with a glycerol concentration in the feeding solution of 100 g/L, and considering a batch volume of 0.25 L, the mass (g) of glycerol to add per hour was:

$$0.25\ L \times 1\ g/L = 0.25\ g/h \quad (7)$$

Since the glycerol concentration in the feed was 100 g/L, the volume of feeding solution to add per hour was:

$$\frac{0.25\ g}{100\ g/L} = 2.5\ mL \quad (8)$$

According to the peristaltic pumps' capacities (mL/h), the velocity needed to meet the desired glycerol feeding rate was set.

For higher glycerol feeding rates, higher velocities were needed, and glycerol concentration in the feeding solution was heightened in order to maintain a low volume of prepared feeding solution.

Table 7 - Glycerol and tryptone concentrations for the three constant feeds.

	Feeding rates (g glycerol/L/h)		
	1	3	6
Glycerol (g/L)	100	200	400
Tryptone (g/L)	80	80	80

For these assays, the three feeding rates were tested as duplicates (A and B), without induction, so that the growth profiles could be established (Figures 15, 16 and 17). In these

fed-batch experiences, glycerol was measured as mentioned in subsection 2.2.4 until the end of the feeding process (Tables 8 and 9).

Table 8 - Glycerol concentration in the medium after starting of the feeding process for the first replicates.

hours after starting of the feeding	Glycerol (g/L)		
	1 g/L/h	3 g/L/h	6 g/L/h
0	6,225552682	5,569737	6,261394
4	0,773322153	3,420133	16,40234
7	0,294115599	1,452985	22,18369
8	0,304508617	0,948538	25,5281
12	0,260855733	0,120626	28,93888

Table 9 - Glycerol concentration in the medium after starting of the feeding process for the second replicates.

hours after starting of the feeding	Glycerol (g/L)		
	1 g/L/h	3 g/L/h	6 g/L/h
0	6,573487913	2,764662	0,045749
2	1,217741049	10,80047	4,615055
4	0,600433918	7,580567	5,239854
6	0,092185485	5,051524	4,969731
8	0,07337344	2,9608	4,921576
10			5,235341
12			6,761802
14			4,8156
16			5,882166

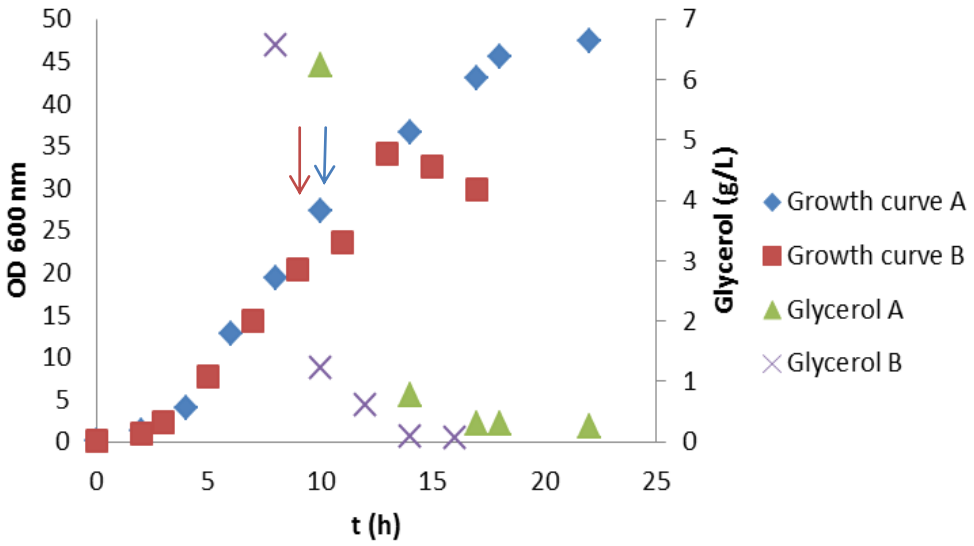

Figure 15 - Growth curves and glycerol concentration profiles of the assays corresponding to 1 g glycerol/L/h. Blue and red arrows indicate the starting of the feeding for replicate A and B, respectively.

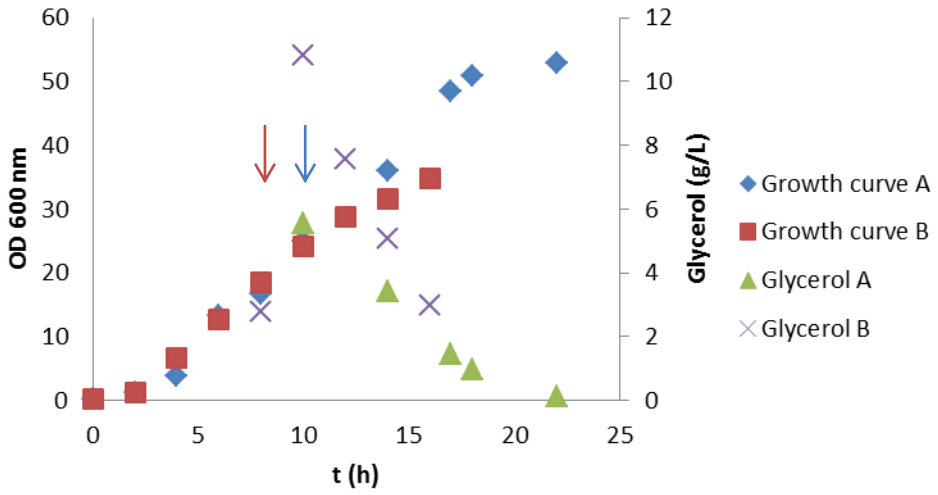

Figure 16 - Growth curves and glycerol concentration profiles of the assays corresponding to 3 g glycerol/L/h. Blue and red arrows indicate the starting of the feeding for replicate A and B, respectively.

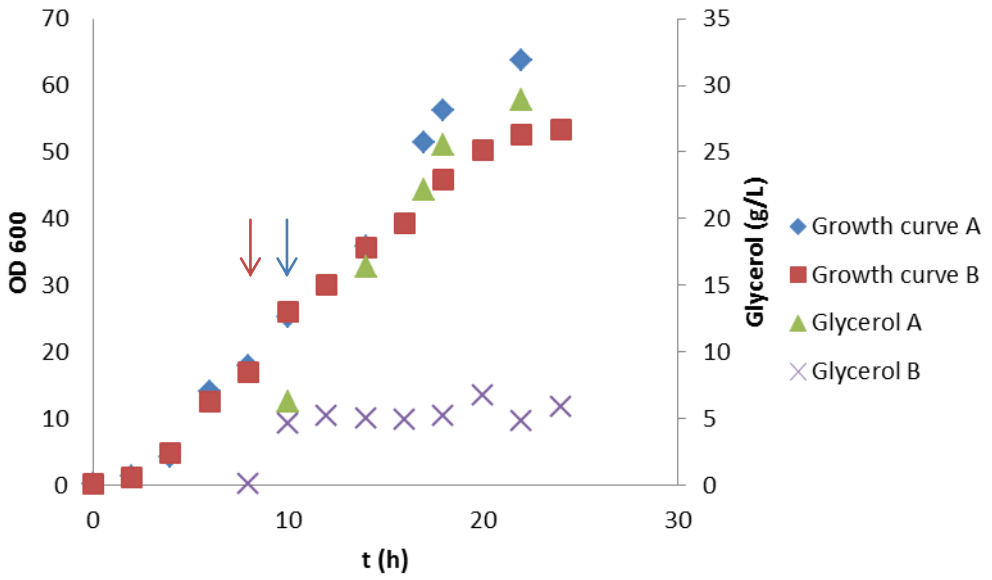

Figure 17 - Growth curves and glycerol concentration profiles of the assays corresponding to 6 g glycerol/L/h. Blue and red arrows indicate the starting of the feeding for replicate A and B, respectively.

From the growth curves, we can see that for all of the feeding profiles, the maximum OD reached was approximately 50 (except for one of the 6 g/L/h assays, which rendered a maximum OD of about 60) which, as expected, are considerably higher than those obtained in the batch experiments.

For the 1 g/L/h constant feeding profile, glycerol concentration at the start of the feeding process was of about 6 g/L for both replicates (probably due to remaining glycerol from the batch phase), and after two hours almost all glycerol was depleted. After that, glycerol concentration was kept close to zero until the end of the fed-batch process, meaning that these cultures were able to consume all of the glycerol provided by the feeding solution, being kept at limiting substrate concentrations during almost all of the feeding process. Nevertheless, for this feeding profile, cells continued growing until a maximum OD of about 50.

For the 3 g/L/h constant feeding profile, the glycerol concentration results of the two replicates are slightly contradictory. Replicate A behaved slightly similarly to 1 g/L/h feeding profiles, presenting a concentration of glycerol at the beginning of the fed-batch phase of about 5.5 g/L. This value also kept decreasing, although not as dramatically as the previous feeding profile. Glycerol concentration reached close to zero values only after about 10 hours of fed-batch, meaning that this feeding profile provides sufficient glycerol concentrations so that limiting concentrations are not reached during most of the fed-batch process. Replicate B behaved differently from replicate A, having a lower (2.76 g/L) glycerol concentration and even increasing that concentration up to 10 g/L after four hours of feeding. After that stage, glycerol concentration kept decreasing (however always staying above the initial concentration of 2.76 g/L) until the end of the process, with a minimum value measured (at

the end of the feeding process) at 2.96 g/L, meaning that cells were not able to consume all the fed glycerol. However, the maximum OD reached (52) was very similar to that of the 1g/L/h feeding profile.

Finally, for the 6 g/L/h feeding profile, results were also discrepant. For the first replicate, the glycerol concentration at the start of the feeding process was relatively high, at 6.26 g/L, probably for the same reasons mentioned before, but also because this fed-batch process was initiated earlier at the batch phase (at 8h). After four hours of fed-batch, glycerol concentration more than doubled, and continued to increase until the end of the process. These results suggest that for this fermentation, the quantity of glycerol fed to the bioreactor was significantly higher than what *E. coli* could consume. For replicate B, however, the starting glycerol concentration for the feeding profile was very close to 0 g/L, and although after four hours it had increased to 5.2 g/L, for the rest of the process it was kept between 5 and 6 g/L, until the end of the fermentation. Nonetheless, the maximum OD reached for this feeding profile was high, 63 for replicate A and 53 for replicate B.

From the three feeding profiles tested, the one that had a greater reproducibility was 1 g/L/h, and since all three of them achieved similar maximum ODs (around 50), this seems the best option from the constant feeding profiles.

Since glycerol concentrations during the fed-batch phase of these three feeding profiles were very different (from almost 0 g/L to as high as 30 g/L), cytometry assays were used to see if the feeding profile of 1 g/L/h is in fact the best choice of the three constant feeding profiles tested.

3.3.1.1 – Cytometry assays

In order to assess cell physiology during the fed-batch experiments, cytometry assays were carried out as described in subsection 2.2.3 (tables 10 and 11). Dead cells will be stained with both BOX and PI, cells with depolarized membrane will be stained only with BOX and viable cells will not be stained.

Table 10 – BOX/PI dual staining results for the first replicates.

hours after starting of the feeding	Percentage of BOX positive and BOX/PI positive cells					
	1 g/L/h		3 g/L/h		6 g/L/h	
0			BOX positive	8,70%	BOX positive	3,80%
			BOX/PI positive	6,88%	BOX/PI positive	5,76%
4	BOX positive	8,30%	BOX positive	7,48%	BOX positive	3,68%
	BOX/PI positive	10,76%	BOX/PI positive	17%	BOX/PI positive	8,36%
8	BOX positive	10,96%	BOX positive	9,24%	BOX positive	7,62%
	BOX/PI positive	18,18%	BOX/PI positive	24,92%	BOX/PI positive	16,08%

Table 11 - BOX/PI dual staining results for the second replicates.

hours after starting of the feeding	Percentage of BOX positive and BOX/PI positive cells					
	1 g/L/h		3 g/L/h		6 g/L/h	
4	BOX positive	4,52 %	BOX positive	3,54 %	BOX positive	8,20%
	PI/BOX positive	3,64 %	PI/BOX positive	3,30 %	PI/BOX positive	6,06%
8	BOX positive	7,74 %			BOX positive	14,36 %
	PI/BOX positive	4,26 %			PI/BOX positive	10,72 %

As the results show, the further the culture progresses in the feeding processes, the more dead cells exist in the culture (probably due to toxic by-products accumulation [45], [46], [53] and prolonged cultivation times), and this effect is heightened at higher feeding rates (possibly because of the higher glycerol concentrations, that can hamper *E. coli* growth).

3.3.2 – Exponential feeding profiles

As mentioned in subsection 1.4.2, exponential feeding allows cells to grow at predetermined specific growth rates, usually between 0.1 and 0.3 h^{-1}, that can be set to fall below the maximum specific growth rate, thus minimizing acetate formation (a growth limiting by-product for *E. coli*) [45, 51].

So, the three chosen specific growth rates for exponential feeding profiles were 0.1, 0.2 and 0.3 h^{-1}, and glycerol and tryptone concentrations in the feeds were the same for all fermentations (400 g/L glycerol and 80 g/L tryptone). To maintain these growth rates, the feeding speed was calculated via equation (9), based on [45].

$$F(t) = \frac{\mu \times Xb \times Vb}{St \times Yx/s} \times e^{\mu t} \quad (9)$$

where F(t) corresponds to feeding speed (L/h), μ is the desired specific growth rate (h^{-1}), X_b is the biomass concentration at the end of the batch phase (g dcw/L), V_b is the initial volume of the fed-batch (L), S_f is the substrate concentration in the feed (g/L), $Y_{X/S}$ is the biomass to substrate yield (specific for each strain, in this case 0.22 g/g [40]) and t the time after the initiation of the feeding (h).

For this set of experiments, the three specific growth rates were also performed in duplicates (A and B) without induction (Figures 18, 19 and 20; Tables 12 and 13). Glycerol quantitation and for flow cytometry assays were performed as they were for the continuous feeding profiles.

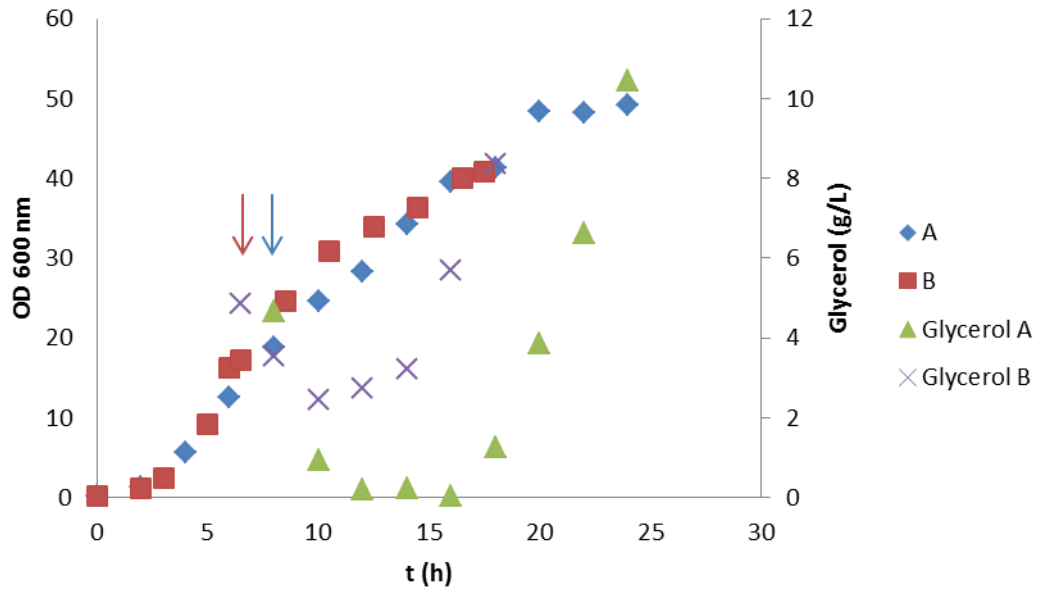

Figure 18 - Growth curves and glycerol concentration profiles of the assays corresponding to 0.1 h^{-1}. Blue and red arrows indicate the starting of the feeding for replicates A and B, respectively.

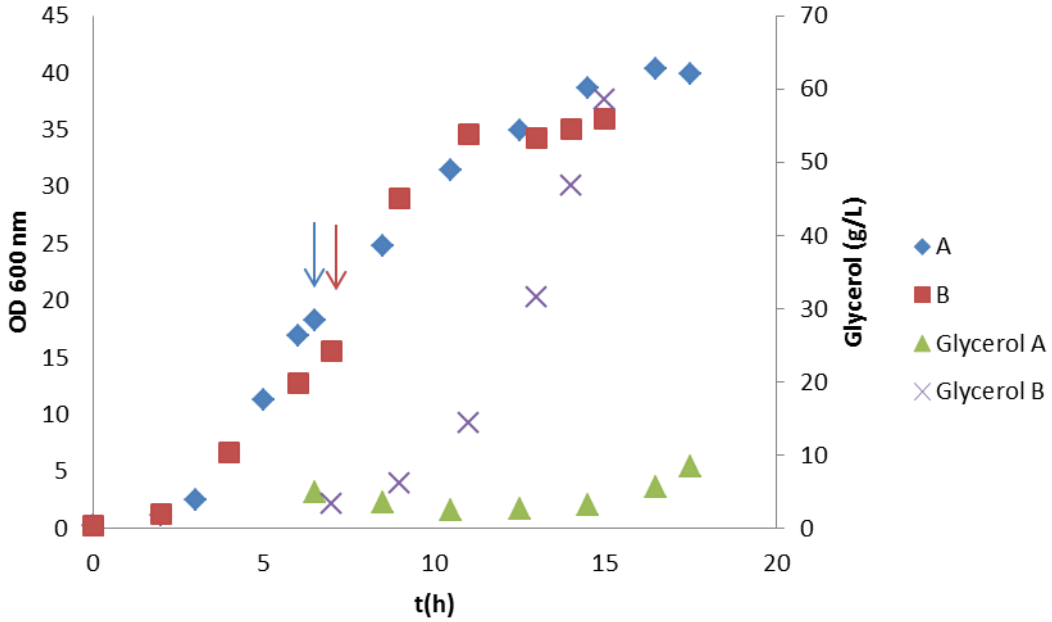

Figure 19 - Growth curves and glycerol concentration profiles of the assays corresponding to 0.2 h^{-1}. Blue and red arrows indicate the starting of the feeding for replicates A and B, respectively.

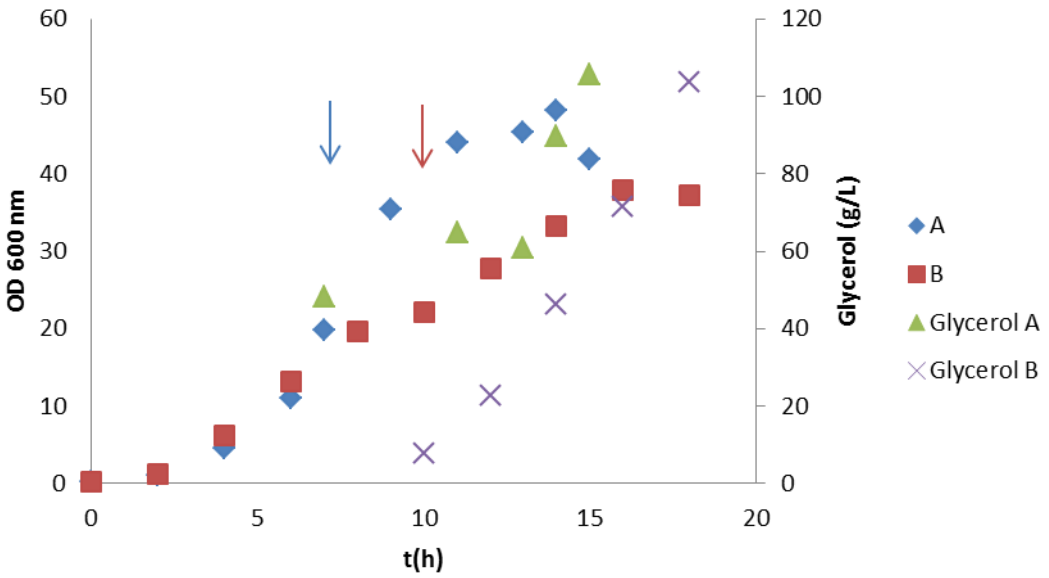

Figure 20 - Growth curves and glycerol concentration profiles of the assays corresponding to 0.3 h^{-1}. Blue and red arrows indicate the starting of the feeding for replicates A and B, respectively.

Table 12 - Glycerol concentration in the medium after starting of the exponential feeding process for the first fermentations.

hours after starting of the feeding	Glycerol (g/L)		
	0.1 h^{-1}	0.2 h^{-1}	0.3 h^{-1}
0	4,648269172	0,4372327	48,13627
2	0,938050331	9,9625895	64,89518
4	0,20828047	24,0902	60,77724
6	0,214551677	42,748891	89,73145
8	0,022346862	51,888771	105,6535
10	1,270643471	67,31168	
12	3,862334364	81,303748	
14	6,620307242		
16	10,44238929		

Table 13 - Glycerol concentration in the medium after starting of the exponential feeding process for the second fermentations.

hours after starting of the feeding	Glycerol (g/L)		
	0.1 h^{-1}	0.2 h^{-1}	0.3 h^{-1}
0	4,85217446	3,438169	7,704565
2	3,541791717	6,1829593	22,6598
4	2,43496897	14,466471	46,34616
6	2,734969965	31,579307	71,37023
8	3,211774856	46,76549	103,5995
10	5,70378154	58,476432	
12	8,370656758		

The results show that for all three specific growth rates tested give approximately the same maximum OD, between 40 and 50, and also similar to those obtained with the constant feeds.

In the first replicate, for a growth rate of 0.1 h^{-1}, glycerol concentration in the medium is kept at low values for the first hours of the exponential feed, but later in the fermentation, it suffered an increase, suggesting that at first, cells were capable of consuming the provided glycerol, but as the feeding speed increases, glycerol starts to accumulate in the medium. For the second replicate, the results were similar to those of the first replicate, but glycerol concentrations did not fall to such low levels, probably because of the fact that the fed-batch process was initiated earlier in the fermentation, and the cells could not account for the glycerol from the feeding solution plus the glycerol that possibly remained from the batch process.

For growth rates of 0.2 and 0.3 h^{-1}, glycerol concentrations are extremely high right from the start of the feeding, due to the high feeding speeds, indicating that cells are not able to exhaust all the glycerol added to the fermentations. However, cell growth was not visibly hampered by these high glycerol levels, as these feeding profiles were able to achieve the same level of OD of that obtained with a growth rate of 0.1 h^{-1}.

From the three previously defined growth rates, the lower rate used (0.1 h^{-1}) seems to be the most attractive, taking into account its reproducibility and the ability demonstrated by the cells to consume the glycerol provided by the feed.

Comparing these results to those obtained with the constant feeds, both techniques achieved very similar maximum ODs (between 50 and 60, approximately), and because the feeding

solutions for the exponential feeds require much larger quantities of glycerol, constant feeds seem preferable, taking into account the lower costs associated.

3.3.2.1 – Cytometry assays

Cytometry assays were performed to assess cell viability during the exponential feeding profiles (Tables 14 and 15)

Table 14 - Cytometry results after starting of the exponential feeding process for the first replicates.

hours after starting of the feeding	Percentage of BOX positive and BOX/PI positive cells					
	0.1 h^{-1}		0.2 h^{-1}		0.3 h^{-1}	
0			BOX positive	12,86%	BOX positive	18,14%
			PI/BOX positive	5,86%	PI/BOX positive	3,12%
4	BOX positive	13,56%	BOX positive	17,58%	BOX positive	15,10%
	PI/BOX positive	5,36%	PI/BOX positive	6,24%	PI/BOX positive	10,66%
8	BOX positive	13,58%				
	PI/BOX positive	6,60%				
12	BOX positive	14,98%				
	PI/BOX positive	7,74%				

Table 15 - Cytometry results after starting of the exponential feeding process for the second replicates.

hours after starting of the feeding	Cytometry percentages					
	1 g/L/h		3 g/L/h		6 g/L/h	
0	BOX positive	4,78%	BOX positive	9,28%	BOX positive	6,57%
	PI/BOX positive	3,14%	PI/BOX positive	2,06%	PI/BOX positive	3,43%
4	BOX positive	9,28%	BOX positive	10,80%	BOX positive	7,62%
	PI/BOX positive	3,24%	PI/BOX positive	3,64%	PI/BOX positive	4,18%
8	BOX positive	9,82%	BOX positive	10,74%		
	PI/BOX positive	3,34%	PI/BOX positive	8,22%		

Just like in constant feeding experiments, cytometry results in exponential feeding show that with the advancing of the feeding process, the number of dead cells increases, as the number of viable cells diminishes.

Glycerol concentration does not seem to have a great influence in cell growth and viability, as the flow cytometry results for the exponential feeding experiments are, in general, lower than those obtained for the constant feeds. If glycerol did have a noticeable effect in cell growth and viability, the high concentrations of glycerol present during the exponential feeds would increase the number of dead and permeabilized cells.

It seems that other aspect may be affecting cell growth in late stages of the fermentation. One of the possibilities is the accumulation of toxic byproducts during the process, that has been reported to happen in fed-batch processes [45, 46, 57]. Another possible factor that might be influencing these results is tryptone concentration, which might be hampering *E. coli* viability as a limiting substrate. At the start of the fermentations, tryptone concentration in the semidefined medium is of 20 g/L, and in the feeding solutions, tryptone was kept constant at 80 g/L. In constant feeding profiles, feed rates are relatively slow, and the amount of tryptone added to the culture is not high. So, towards the end of the fermentations, tryptone might have been depleted, which might help explaining the higher amount of dead and depolarized cells in these processes, in comparison with the exponential feeds that had much greater feeding speeds providing fresh tryptone to the cultures.
Taking into account the results of both feeding profiles, and for the reasons mentioned above, the selected feeding profile for hSCOMT induction fermentation was a constant feed of 1 g glycerol/L/h.

3.4 - COMT production in fed-batch fermentations

As mentioned above, for the final fermentations a constant feed of 1 g glycerol/L/h was used, with a higher (50 g/L) initial concentration of tryptone in order to compensate the possible tryptone limitation during the fed-batch phase. All other process conditions remained unaltered.

Firstly, a fermentation without induction was performed, in order to determine the starting of the stationary phase with this new medium formulation, and consequently the starting of the feeding (Figure 21).

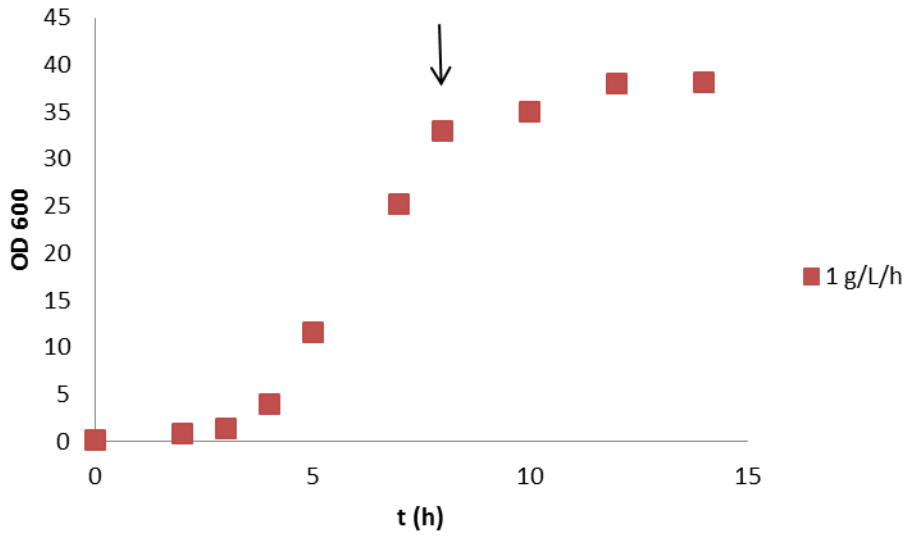

Figure 21 - Growth curve of the 1 g/L/h fermentation, with 50g/L of initial tryptone concentration. The arrow indicates the starting of the feeding.

As seen in Figure 21, the stationary phase was reached at about 8 hours into the fermentation, and that was the time chosen to initiate the feeding. However, and since there was no significant increase in cell growth after this point, we decided to initiate the feeding one hour earlier (at 7h) in the subsequent experiment, with IPTG induction (Figure 22). According to previously described data [40], the induction was carried out 1 hour after starting of the feeding, for four hours.

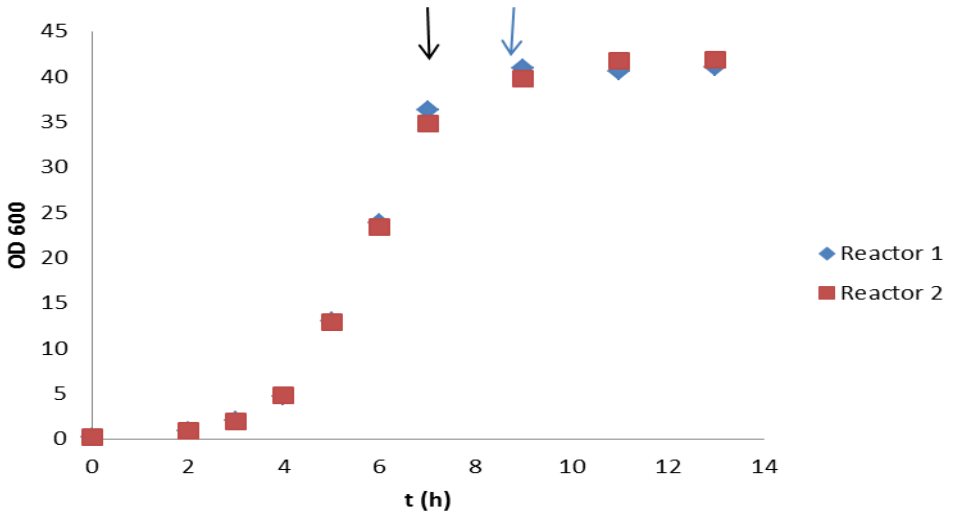

Figure 22 - Growth curve for the final fermentation, with IPTG induction. Black and blue arrows indicate the starting of the feeding and induction time, respectively.

For this fermentation, glycerol quantitation assays were carried out as mentioned above (chromatogram demonstrated in figure 23). The correspondent glycerol peak (elution time of about 13.5 min) was manually integrated and the resulting area used to calculate glycerol concentration. All other samples were treated in the same way.

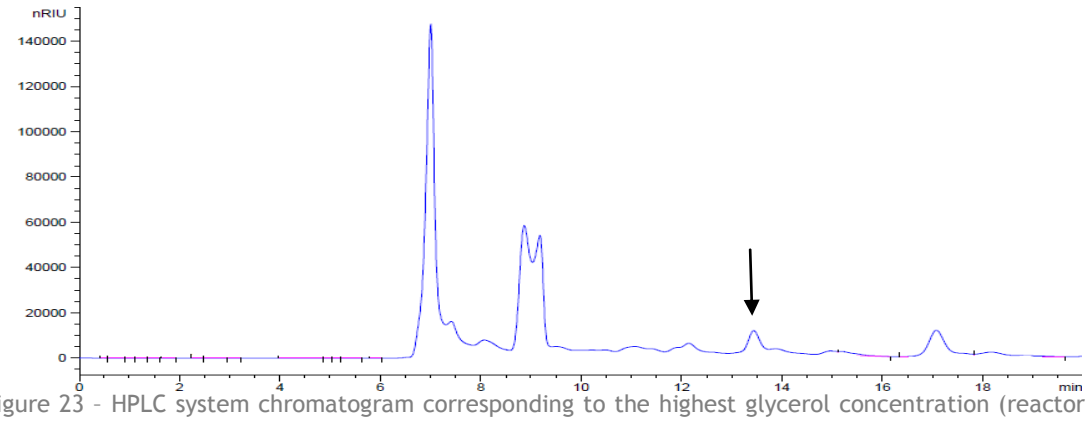

Figure 23 – HPLC system chromatogram corresponding to the highest glycerol concentration (reactor 1, 0h). Glycerol has an elution time of about 13.5 min (black arrow).

Table 16 - Glycerol concentration after feeding initiation, for both replicates.

hours after feeding initiation	Glycerol (g/L)	
	Reactor 1	Reactor 2
0	0,515463199	0,325127526
2	0,52729217	0,296274455
4	0,066608735	0,374067381
6	0,069458567	0,31511961

As expected, glycerol consumption profile was very similar to the previous assays carried out with this feeding profile, however in this case, glycerol concentration was low just from the beginning, and after two hours of feeding, the concentrations remained the same in both replicates. Maximum OD reached in these fermentations was a little lower (about 40), which can be associated with IPTG induction, since this inducer is known to be toxic and promote metabolic stress [42, 47].

3.4.1- Cytometry assay

Cytometry assays were carried out as explained above, and the results for these fermentations can be seen in figure 24 (only for the first replicate). Other replicate's samples were treated in the same way and results are shown in table 17.

Dead cells will be stained with both BOX and PI, cells with depolarized membrane will be stained only with BOX and viable cells will not be stained.

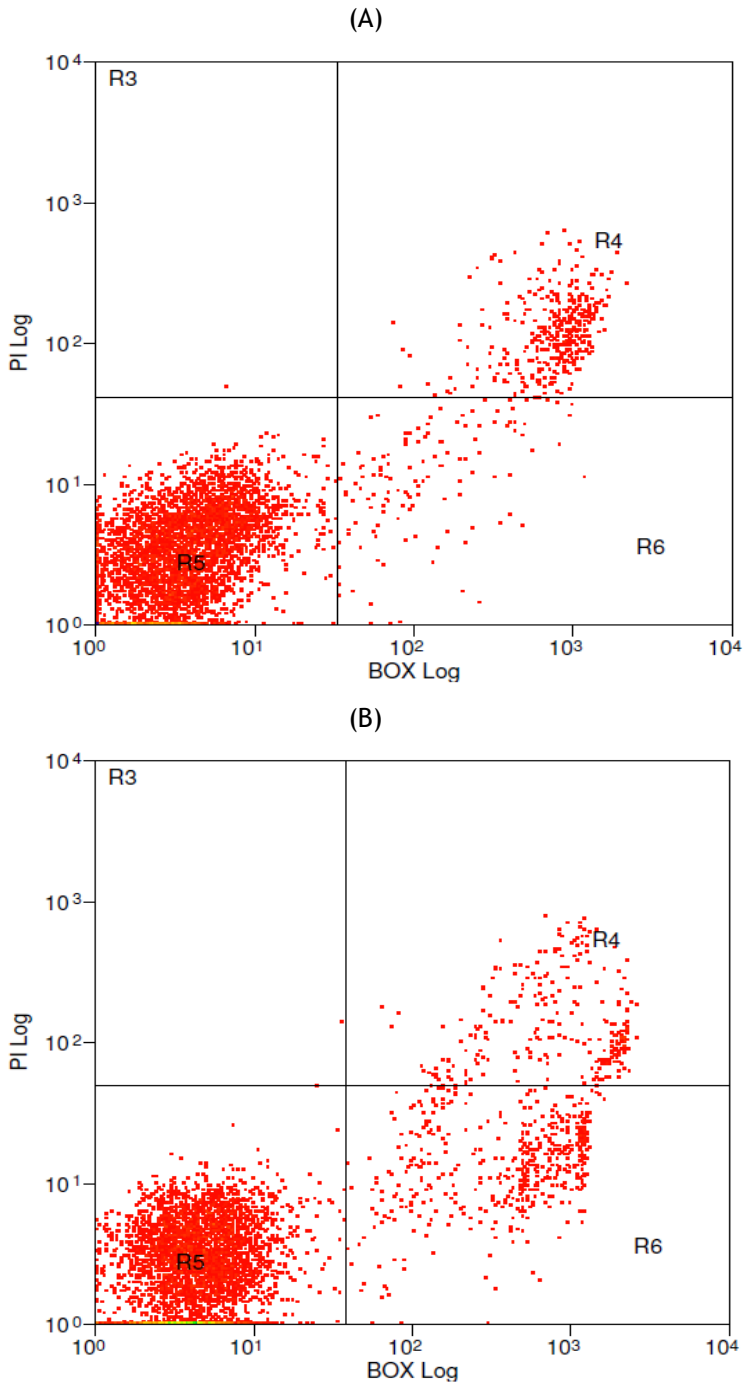

Figure 24 - Cell samples taken at (A) 0h immediately after induction and (B) 4h after induction, for the first replicate. Cells were stained with PI/BOX, and up to three main subpopulations of cells can be distinguished, corresponding to healthy polarized cells (R5), not stained; depolarized cells (R6), stained with BOX; and cells with permeabilized and depolarized cytoplasmatic membranes, (R4), stained with both PI and BOX.

Table 17 - Cytometry results after starting of the exponential feeding process for both replicates (reactor 1 and reactor 2).

hours after starting of the feeding	Percentage of BOX positive and BOX/PI positive cells			
	Reactor 1		Reactor 2	
0	BOX positive	2,56%	BOX positive	3,80%
	PI/BOX positive	8,02%	PI/BOX positive	7,54%
4	BOX positive	5,66%	BOX positive	3,30%
	PI/BOX positive	10,28%	PI/BOX positive	12,50%

The comparison of cytometry results from the fermentations at constant feeding with the same feeding rate (1g/L/h) showed overall lower percentages of permeabilized and dead cells. This may possibly be due to the higher concentration of tryptone present in these fermentations, confirming the above mentioned possible effect of low concentrations of tryptone in cell viability.

Another reason for these seemingly better results might be process duration. In these last assays, the whole process (batch and fed-batch) only took 13 hours to develop, against the 17 and 22 hours of the processes that used the same feeding rate. This shorter period was probably due to the early implementation of the fed-batch technique (7 hours of batch fermentation, against 9 and 10 for the other assays). With lower process durations, possibly toxic by-products are less likely to accumulate, or they do so at lower levels, and so their effect on cell viability is not so evident.

3.4.2 – Enzymatic assay

For enzymatic assay, samples were taken every 2 hours after induction, and treated according to the method described in subsection 2.2.7 (exemplificative chromatogram in figure 24) resulting in the specific activity values depicted in Table 18.

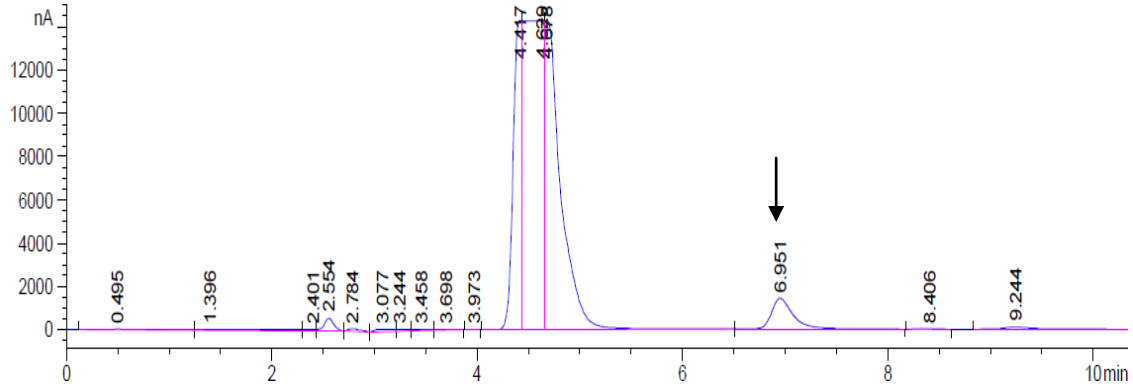

Figure 25 – HPLC system chromatogram for the highest specific activity sample (4 hours after induction). Metanephrine has an elution time of about 6.9 minutes (black arrow).

The peak correspondent to metanephrine (6.9 minutes of elution time) was manually integrated, and the area value used to calculate specific hSCOMT activity, as described above. The same procedure was applied to all other samples (Table 17).

Table 18 - Specific activity values for both replicates.

hours after induction	Specific activity (nmol/h/mg)	
	Reactor 1	Reactor 2
2	58,05106334	56,83245922
4	292,2498991	-
6	442,3415365	379,4840643

As the results show, specific enzymatic activity enhances progressively after induction, with the highest value (442.34 nmol/h/mg) being achieved 6 hours after induction, since the promoter had more time to act. However, if the culture were to be maintained for more time, this increment in specific activity would probably cease, because over that period of time the protein would lose its activity (due to the adverse conditions in the culture).

Chapter 4 - Conclusions

Human SCOMT has received an increasing interest in the past years due to its implication in several neurodegenerative diseases, particularly in Alzheimer's and Parkinson's diseases. As one of the most important enzymes in dopamine breakdown, the development of COMT inhibitors can be seen as one of the most promising therapeutical approaches for these diseases as the inhibition of COMT activity and the inherent inhibition of dopamine breakdown, can lead to an increase of its levels in the brain.

Currently available COMT inhibitors are divided into first and second generation inhibitors, First generation COMT inhibitors were found very short acting and toxic, and also to have low efficacy *in vivo* and selectivity, while second generation COMT inhibitors are either less effective, or have a high toxicity risk. These two generations do not meet therapeutic demands, and so new COMT inhibitors are a promising field of research.

However, to develop new COMT inhibitors, high quantities of enzymatically active protein are needed, making the design of an effective production process for this enzyme highly relevant in order to achieve this aim. Some research has been done in this field, but few scale-up processes have been established.

In this study, several fermentation conditions were tested to increase SCOMT production in *E. coli* BL21 (DE3) strains, with the objective of developing a fed-batch strategy suitable for COMT production.

First, a batch process was tested as a ground layer for further production enhancement experiments. Three different dissolved oxygen percentages were tested in duplicates to determine the best one to proceed with the studies, in a series of 6 batch experiments. The selected value was 20%, and this experiment was repeated with induction for a basis of enzymatic activity to be achieved. In this step, a maximum specific COMT activity of 316.16 nmol/h/mg was achieved.

The second step in this study was to define carbon and nitrogen sources concentrations in the batch-phase of the fed-batch fermentations to decrease batch duration, allowing the final fed-batch process to be more efficient. This was achieved by manipulating the amount of nitrogen and carbon sources in the medium, allowing the stationary phase of bacterial growth to be achieved earlier in the fermentation. Three different formulations were tested in a set of three experiments, and the selected medium contained a glycerol and tryptone concentration of 20 g/L.

Then, two fed-batch strategies were tested (constant and exponential feeding) with three different feeding profiles for each one of them being developed, in a total of 12 fed-batch experiments. Based in maximum optical density reached, glycerol consumption and cell viability, the chosen feeding profile was fixed to a constant feed of 1 g glycerol/L/h.

Given the best option for feeding profile, it was tested in duplicate in a final experiment, being induced to achieve a maximum total COMT activity of 66.35 nmol/h. In a preliminary study developed by this research group, a total hSCOMT activity of 183.73 nmol/h was achieved. A fed-batch process developed by the same research group obtained a best result of hSCOMT activity of 581.78 U/L.

This study indicates that a fed-batch process as a good option for recombinant human SCOMT production in *E. coli* BL21 (DE3), and it was verified that a constant feeding process is preferable to exponential feeding strategies. Also, a great increment in cell density was achieved (compared to a previous work on a fed-batch process for this system by this research group) only by applying previously optimized parameters from small scale fermentations, at first, and later by changing medium composition and feeding strategies. This suggests that further optimization of this particular expression system is a great option for human SCOMT production scale-up, and should give even better results in terms of cell growth and protein productivity.

Chapter 5 – Bibliography

[1] J. Axelrod and R. Tomchick, "Enzymatic O-Methylation of Epinephrine and Other Catechols," *J. Biol. Chem.*, vol. 233, no. 3, pp. 702–705, Sep. 1958.

[2] J. Axelrod, S. Senoh, and B. Witkop, "O-Methylation of Catechol Amines in Vivo," *J. Biol. Chem.*, vol. 233, no. 3, pp. 697–701, Sep. 1958.

[3] P. T. Mannisto and S. Kaakkola, "Catechol-O-methyltransferase (COMT): Biochemistry, Molecular Biology, Pharmacology, and Clinical Efficacy of the New Selective COMT Inhibitors," *Pharmacol. Rev.*, vol. 51, no. 4, pp. 593–628, Dec. 1999.

[4] K. Rutherford, I. Le Trong, R. E. Stenkamp, and W. W. Parson, "Crystal structures of human 108V and 108M catechol O-methyltransferase.," *Journal of molecular biology*, vol. 380, no. 1, pp. 120–30, Jun. 2008.

[5] E. M. Tunbridge, P. J. Harrison, and D. R. Weinberger, "Catechol-o-methyltransferase, cognition, and psychosis: Val158Met and beyond.," *Biological psychiatry*, vol. 60, no. 2, pp. 141–51, Jul. 2006.

[6] M. Flirski, T. Sobow, and I. Kloszewska, "Behavioural genetics of Alzheimer's disease: a comprehensive review.," *Archives of medical science : AMS*, vol. 7, no. 2, pp. 195–210, Apr. 2011.

[7] K. Rutherford, E. Alphandéry, a McMillan, V. Daggett, and W. W. Parson, "The V108M mutation decreases the structural stability of catechol O-methyltransferase.," *Biochimica et biophysica acta*, vol. 1784, no. 7–8, pp. 1098–105, 2008.

[8] B. Borroni, M. Grassi, C. Agosti, C. Costanzi, S. Archetti, S. Franzoni, C. Caltagirone, M. Di Luca, L. Caimi, and a Padovani, "Genetic correlates of behavioral endophenotypes in Alzheimer disease: role of COMT, 5-HTTLPR and APOE polymorphisms.," *Neurobiology of aging*, vol. 27, no. 11, pp. 1595–603, Nov. 2006.

[9] S. Wedren, "Catechol-O-methyltransferase gene polymorphism and post-menopausal breast cancer risk," *Carcinogenesis*, vol. 24, no. 4, pp. 681–687, Apr. 2003.

[10] M. Karayiorgou, M. Altemus, B. L. Galke, D. Goldman, D. L. Murphy, J. Ott, and J. a Gogos, "Genotype determining low catechol-O-methyltransferase activity as a risk factor for obsessive-compulsive disorder.," *Proceedings of the National Academy of Sciences of the United States of America*, vol. 94, no. 9, pp. 4572–5, Apr. 1997.

[11] H. M. Lachman, K. a Nolan, P. Mohr, T. Saito, and J. Volavka, "Association between catechol O-methyltransferase genotype and violence in schizophrenia and schizoaffective disorder.," *The American journal of psychiatry*, vol. 155, no. 6, pp. 835–7, Jun. 1998.

[12] R. D. Strous, N. Bark, S. S. Parsia, J. Volavka, and H. M. Lachman, "Analysis of a functional catechol-O-methyltransferase gene polymorphism in schizophrenia: evidence for association with aggressive and antisocial behavior.," *Psychiatry research*, vol. 69, no. 2–3, pp. 71–7, Mar. 1997.

[13] L. Diatchenko, G. D. Slade, A. G. Nackley, K. Bhalang, A. Sigurdsson, I. Belfer, D. Goldman, K. Xu, S. a Shabalina, D. Shagin, M. B. Max, S. S. Makarov, and W. Maixner, "Genetic basis for individual variations in pain perception and the development of a

chronic pain condition.," *Human molecular genetics*, vol. 14, no. 1, pp. 135–43, Jan. 2005.

[14] T. E. Goldberg, M. F. Egan, T. Gscheidle, and R. Coppola, "Executive Subprocesses in Working Memory," vol. 60, 2003.

[15] M. J. Bonifácio, M. Archer, M. L. Rodrigues, P. M. Matias, D. a Learmonth, M. A. Carrondo, and P. Soares-Da-Silva, "Kinetics and crystal structure of catechol-o-methyltransferase complex with co-substrate and a novel inhibitor with potential therapeutic application.," *Molecular pharmacology*, vol. 62, no. 4, pp. 795–805, Oct. 2002.

[16] J. L. Martin and F. M. McMillan, "SAM (dependent) I AM: the S-adenosylmethionine-dependent methyltransferase fold.," *Current opinion in structural biology*, vol. 12, no. 6, pp. 783–93, Dec. 2002.

[17] J. a Gogos, M. Morgan, V. Luine, M. Santha, S. Ogawa, D. Pfaff, and M. Karayiorgou, "Catechol-O-methyltransferase-deficient mice exhibit sexually dimorphic changes in catecholamine levels and behavior.," *Proceedings of the National Academy of Sciences of the United States of America*, vol. 95, no. 17, pp. 9991–6, Aug. 1998.

[18] E. M. Tunbridge, D. M. Bannerman, T. Sharp, and P. J. Harrison, "Catechol-o-methyltransferase inhibition improves set-shifting performance and elevates stimulated dopamine release in the rat prefrontal cortex.," *The Journal of neuroscience : the official journal of the Society for Neuroscience*, vol. 24, no. 23, pp. 5331–5, Jun. 2004.

[19] B. Borroni, M. Grassi, C. Costanzi, M. Zanetti, S. Archetti, S. Franzoni, L. Caimi, and a Padovani, "Haplotypes in cathechol-O-methyltransferase gene confer increased risk for psychosis in Alzheimer disease.," *Neurobiology of aging*, vol. 28, no. 8, pp. 1231–8, Aug. 2007.

[20] R. C. Brown, A. H. Lockwood, and B. R. Sonawane, "Neurodegenerative Diseases: An Overview of Environmental Risk Factors," *Environmental Health Perspectives*, vol. 113, no. 9, pp. 1250–1256, May 2005.

[21] V. Ramanan and A. Saykin, "Pathways to neurodegeneration: mechanistic insights from GWAS in Alzheimer's disease, Parkinson's disease, and related disorders," … *journal of neurodegenerative disease*, vol. 2, no. 3, pp. 145–175, 2013.

[22] D. Blacker, B. F. Boeve, J. D. Bowen, A. Boxer, J. R. Burke, G. Cai, N. J. Cairns, C. Cao, C. S. Carlson, R. M. Carney, S. L. Carroll, H. C. Chui, D. G. Clark, D. H. Cribbs, E. A. Crocco, C. Cruchaga, C. Decarli, S. T. Dekosky, F. Y. Demirci, M. Dick, K. M. Faber, K. B. Fallon, M. R. Farlow, S. Ferris, M. P. Frosch, D. R. Galasko, M. Ganguli, M. Gearing, D. H. Geschwind, N. W. Kowall, J. H. Kramer, P. Kramer, F. M. Laferla, J. J. Lah, R. Lang-walker, J. B. Leverenz, D. C. Mash, E. Masliah, W. C. Mccormick, S. M. Mccurry, A. N. Mcdavid, and A. C. Mckee, "Variants in the ATP-binding cassette transporter (ABCA7), apolipoprotein E ϵ4,and the risk of late-onset Alzheimer disease in African Americans.," vol. 309, no. 14, pp. 1483–1492, 2013.

[23] V. Licker, E. Kövari, D. F. Hochstrasser, and P. R. Burkhard, "Proteomics in human Parkinson's disease research.," *Journal of proteomics*, vol. 73, no. 1, pp. 10–29, Nov. 2009.

[24] R. a Sweet, B. Devlin, B. G. Pollock, D. L. Sukonick, K. B. Kastango, S. Bacanu, K. V Chowdari, S. T. DeKosky, and R. E. Ferrell, "Catechol-O-methyltransferase haplotypes are associated with psychosis in Alzheimer disease.," *Molecular psychiatry*, vol. 10, no. 11, pp. 1026–36, Nov. 2005.

[25] B. Thomas and M. F. Beal, “Parkinson’s disease.,” *Human molecular genetics*, vol. 16 Spec No, no. 2, pp. R183–94, Oct. 2007.

[26] “S . 13 Parkinson ’ s disease : novel treatment strategies,” pp. 87–88, 1981.

[27] D. Salat and E. Tolosa, “Levodopa in the treatment of Parkinson’s disease: current status and new developments.,” *Journal of Parkinson’s disease*, vol. 3, no. 3, pp. 255–69, Jan. 2013.

[28] M. J. Bonifácio, P. N. Palma, L. Almeida, and P. Soares-da-Silva, “Catechol-O-methyltransferase and its inhibitors in Parkinson’s disease.,” *CNS drug reviews*, vol. 13, no. 3, pp. 352–379, 2007.

[29] R. Talati, K. Reinhart, W. Baker, C. M. White, and C. I. Coleman, “Pharmacologic treatment of advanced Parkinson’s disease: a meta-analysis of COMT inhibitors and MAO-B inhibitors.,” *Parkinsonism & related disorders*, vol. 15, no. 7, pp. 500–5, Aug. 2009.

[30] R. Pahwa, S. a Factor, K. E. Lyons, W. G. Ondo, G. Gronseth, H. Bronte-Stewart, M. Hallett, J. Miyasaki, J. Stevens, and W. J. Weiner, “Practice Parameter: treatment of Parkinson disease with motor fluctuations and dyskinesia (an evidence-based review): report of the Quality Standards Subcommittee of the American Academy of Neurology.,” *Neurology*, vol. 66, no. 7, pp. 983–95, Apr. 2006.

[31] C. Chakraborty, S. Pal, C. G. P. Doss, Z.-H. Wen, and C.-S. Lin, “In silico analyses of COMT, an important signaling cascade of dopaminergic neurotransmission pathway, for drug development of Parkinson’s disease.,” *Applied biochemistry and biotechnology*, vol. 167, no. 4, pp. 845–60, Jun. 2012.

[32] L. E. Kiss, H. S. Ferreira, L. Torrão, M. J. Bonifácio, P. N. Palma, P. Soares-da-Silva, and D. a Learmonth, “Discovery of a long-acting, peripherally selective inhibitor of catechol-O-methyltransferase.,” *Journal of medicinal chemistry*, vol. 53, no. 8, pp. 3396–411, Apr. 2010.

[33] F. Assal, L. Spahr, a Hadengue, L. Rubbia-Brandt, P. R. Burkhard, and L. Rubbici-Brandt, “Tolcapone and fulminant hepatitis.,” *Lancet*, vol. 352, no. 9132. p. 958, 19-Sep-1998.

[34] Z. Ma, H. Liu, and B. Wu, “Structure-based drug design of catechol-O-methyltransferase inhibitors for CNS disorders.,” *British journal of clinical pharmacology*, May 2013.

[35] I. Ulmanen, J. Peränen, J. Tenhunen, C. Tilgmann, T. Karhunen, P. Panula, L. Bernasconi, J. P. Aubry, and K. Lundström, “Expression and intracellular localization of catechol O-methyltransferase in transfected mammalian cells.,” *European journal of biochemistry / FEBS*, vol. 243, no. 1–2, pp. 452–9, Jan. 1997.

[36] C. Tilgmann, K. Melen, K. Lundström, a Jalanko, I. Julkunen, N. Kalkkinen, and I. Ulmanen, “Expression of recombinant soluble and membrane-bound catechol O-methyltransferase in eukaryotic cells and identification of the respective enzymes in rat brain.,” *European journal of biochemistry / FEBS*, vol. 207, no. 2, pp. 813–21, Jul. 1992.

[37] J. Kelloniemi, K. Mäkinen, and J. P. T. Valkonen, “A potyvirus-based gene vector allows producing active human S-COMT and animal GFP, but not human sorcin, in vector-infected plants.,” *Biochimie*, vol. 88, no. 5, pp. 505–13, May 2006.

[38] H.-W. Bai, J.-Y. Shim, J. Yu, and B. T. Zhu, “Biochemical and molecular modeling studies of the O-methylation of various endogenous and exogenous catechol substrates catalyzed by recombinant human soluble and membrane-bound catechol-O-methyltransferases.,” *Chemical research in toxicology*, vol. 20, no. 10, pp. 1409–25, Oct. 2007.

[39] R. Silva, S. Ferreira, M. J. Bonifácio, J. M. L. Dias, J. a Queiroz, and L. a Passarinha, “Optimization of fermentation conditions for the production of human soluble catechol-O-methyltransferase by Escherichia coli using artificial neural network.,” *Journal of biotechnology*, vol. 160, no. 3–4, pp. 161–8, Aug. 2012.

[40] L. Passarinha, M. Bonifacio, and J. Queiroz, “Application of a fed-batch bioprocess for the heterologous production of hSCOMT in Escherichia coli,” *Journal of microbiology and …*, vol. 19, no. June, 2009.

[41] D. C. Andersen and L. Krummen, “Recombinant protein expression for therapeutic applications.,” *Current opinion in biotechnology*, vol. 13, no. 2, pp. 117–23, Apr. 2002.

[42] F. Baneyx, “Recombinant protein expression in Escherichia coli,” *Current opinion in biotechnology*, 1999.

[43] K. Marisch, K. Bayer, M. Cserjan-Puschmann, M. Luchner, and G. Striedner, “Evaluation of three industrial Escherichia coli strains in fed-batch cultivations during high-level SOD protein production.,” *Microbial cell factories*, vol. 12, no. 1, p. 58, Jan. 2013.

[44] K. Terpe, “Overview of bacterial expression systems for heterologous protein production: from molecular and biochemical fundamentals to commercial systems.,” *Applied microbiology and biotechnology*, vol. 72, no. 2, pp. 211–22, Sep. 2006.

[45] S. Y. Lee, “High cell-density culture of Escherichia coli.,” *Trends in biotechnology*, vol. 14, no. 3, pp. 98–105, Mar. 1996.

[46] J. Shiloach and R. Fass, “Growing E. coli to high cell density--a historical perspective on method development.,” *Biotechnology advances*, vol. 23, no. 5, pp. 345–57, Jul. 2005.

[47] S. Makrides, “Strategies for achieving high-level expression of genes in Escherichia coli.,” *Microbiological reviews*, vol. 60, no. 3, 1996.

[48] O. Khow and S. Suntrarachun, “Strategies for production of active eukaryotic proteins in bacterial expression system.,” *Asian Pacific journal of tropical biomedicine*, vol. 2, no. 2, pp. 159–62, Feb. 2012.

[49] S. Schlegel, J. Löfblom, C. Lee, A. Hjelm, M. Klepsch, M. Strous, D. Drew, D. J. Slotboom, and J.-W. de Gier, “Optimizing membrane protein overexpression in the Escherichia coli strain Lemo21(DE3).,” *Journal of molecular biology*, vol. 423, no. 4, pp. 648–59, Nov. 2012.

[50] T. Collins, J. Azevedo-Silva, A. da Costa, F. Branca, R. Machado, and M. Casal, “Batch production of a silk-elastin-like protein in E. coli BL21(DE3): key parameters for optimisation.,” *Microbial cell factories*, vol. 12, p. 21, Jan. 2013.

[51] D. J. Korz, U. Rinas, K. Hellmuth, E. a Sanders, and W. D. Deckwer, “Simple fed-batch technique for high cell density cultivation of Escherichia coli.,” *Journal of biotechnology*, vol. 39, no. 1, pp. 59–65, Feb. 1995.

[52] F. Silva, J. Queiroz, and F. Domingues, “Plasmid DNA fermentation strategies: influence on plasmid stability and cell physiology,” *Applied microbiology and …*, vol. 93, no. 6, pp. 2571–80, Mar. 2012.

[53] F. Silva, J. a Queiroz, and F. C. Domingues, “Evaluating metabolic stress and plasmid stability in plasmid DNA production by Escherichia coli.,” *Biotechnology advances*, vol. 30, no. 3, pp. 691–708, 2012.

[54] M. Díaz, M. Herrero, L. a. García, and C. Quirós, “Application of flow cytometry to industrial microbial bioprocesses,” *Biochemical Engineering Journal*, vol. 48, no. 3, pp. 385–407, Feb. 2010.

[55] J. O. Konz, J. King, and C. L. Cooney, “Effects of oxygen on recombinant protein expression.,” *Biotechnology progress*, vol. 14, no. 3, pp. 393–409, 1998.

[56] K. Friehs and K. F. Reardon, “Parameters influencing the productivity of recombinant E. coli cultivations.,” *Advances in biochemical engineering/biotechnology*, vol. 48, pp. 53–77, Jan. 1993.

[57] S. Pflug, S. M. Richter, and V. B. Urlacher, “Development of a fed-batch process for the production of the cytochrome P450 monooxygenase CYP102A1 from Bacillus megaterium in E. coli.,” *Journal of biotechnology*, vol. 129, no. 3, pp. 481–8, May 2007.

[58] J. H. Choi, S. J. Lee, and S. Y. Lee, “Enhanced Production of Insulin-Like Growth Factor I Fusion Protein in Escherichia coli by Coexpression of the Down-Regulated Genes Identified by Transcriptome Profiling,” *Applied and Environmental Microbiology*, vol. 69, no. 8, pp. 4737–4742, Aug. 2003.